

AD-A163 782

ELECTROMAGNETIC SCATTERING FROM A SLOTTED TM
CYLINDRICAL CONDUCTOR BY THE. (U) SYRACUSE UNIV NY DEPT
OF ELECTRICAL AND COMPUTER ENGINEERING.

1/1

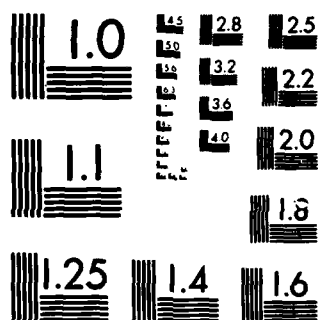
UNCLASSIFIED

J R MAUTZ ET AL. SEP 85 SYRU/DECE/TR-85/3

F/G 28/14

NL

				END								
				FILED								
				UIC								



MICROCOPY RESOLUTION TEST CHART
NATIONAL BUREAU OF STANDARDS-1963-A

AD-A163 782

SYRU/DECE/TR-85/3

ELECTROMAGNETIC SCATTERING FROM A SLOTTED TM CYLINDRICAL
CONDUCTOR BY THE PSEUDO-IMAGE METHOD

Interim Technical Report No. 2

by

Joseph R. Mautz
Xingchao Yuan
Roger F. Harrington

September 1985

Department of
Electrical and Computer Engineering
Syracuse University
Syracuse, New York 13210

Contract No. DAAG29-84-K-0078

Approved for public release; distribution unlimited

Reproduction in whole or in part permitted for any
purpose of the United States Government

Prepared for

ARMY RESEARCH OFFICE
RESEARCH TRIANGLE PARK
NORTH CAROLINA 27709

UNCLASSIFIED

SECURITY CLASSIFICATION OF THIS PAGE (When Data Entered)

REPORT DOCUMENTATION PAGE		READ INSTRUCTIONS BEFORE COMPLETING FORM
1. REPORT NUMBER ARO 21378-3-EL	2. GOVT ACCESSION NO.	3. RECIPIENT'S CATALOG NUMBER
4. TITLE (and Subtitle) ELECTROMAGNETIC SCATTERING FROM A SLOTTED TM CYLINDRICAL CONDUCTOR BY THE PSEUDO-IMAGE METHOD		5. TYPE OF REPORT & PERIOD COVERED Interim Technical Report #2.
		6. PERFORMING ORG. REPORT NUMBER
7. AUTHOR(s) Joseph R. Mautz Xingchao Yuan Roger F. Harrington		8. CONTRACT OR GRANT NUMBER(s) DAAG29-84-K-0078
9. PERFORMING ORGANIZATION NAME AND ADDRESS Department of Electrical & Computer Engineering Syracuse University Syracuse, New York 13210		10. PROGRAM ELEMENT, PROJECT, TASK AREA & WORK UNIT NUMBERS
11. CONTROLLING OFFICE NAME AND ADDRESS U.S. Army Research Office Post Office Box 12211 Research Triangle Park, NC 27709		12. REPORT DATE September 1985
		13. NUMBER OF PAGES 58
14. MONITORING AGENCY NAME & ADDRESS (if different from Controlling Office)		15. SECURITY CLASS. (of this report) UNCLASSIFIED
		15a. DECLASSIFICATION/DOWNGRADING SCHEDULE
16. DISTRIBUTION STATEMENT (of this Report) Approved for public release; distribution unlimited		
17. DISTRIBUTION STATEMENT (of the abstract entered in Block 20, if different from Report) NA		
18. SUPPLEMENTARY NOTES The view, opinions, and/or findings contained in this report are those of the author(s) and should not be construed as an official Department of the Army position, policy, or decision, unless so designated by other documen- tation.		
19. KEY WORDS (Continue on reverse side if necessary and identify by block number) Aperture admittance Pseudo-image method Electromagnetic scattering Slotted cylinder Generalized network formulation Two-dimensional fields		
20. ABSTRACT (Continue on reverse side if necessary and identify by block number) The generalized network formulation for aperture problems is a well- established method for determining electromagnetic scattering from an aperture- perforated conducting surface. This method is easily implemented for an aper- ture in an infinite conducting plane because the field due to a sheet of mag- netic current M on the surface of a conducting plane is, by the method of images, the field of $2M$ in free space. The method is more difficult to im- plement for an aperture in a curved conducting surface because the electric current induced by M on this surface can not be accounted for by imaging.		

DD FORM 1473
1 JAN 73EDITION OF 1 NOV 65 IS OBSOLETE
S/N 0102-014-6601

UNCLASSIFIED

SECURITY CLASSIFICATION OF THIS PAGE (When Data Entered)

UNCLASSIFIED

SECURITY CLASSIFICATION OF THIS PAGE(When Data Entered)

20. ABSTRACT (continued)

This current must be calculated. Its calculated values are often inaccurate and so are those of the aperture field. In the present work, a more accurate aperture field is obtained for a particular TM curved cylindrical surface by means of the generalized network formulation for aperture problems in conjunction with a new method called the pseudo-image method. This aperture field was calculated by means of computer programs which will be described and listed in a forthcoming report. *words - to field 19*

UNCLASSIFIED

SECURITY CLASSIFICATION OF THIS PAGE(When Data Entered)

CONTENTS

	Page
I. INTRODUCTION-----	1
II. STATEMENT OF THE PROBLEM-----	4
III. SOLUTION BY THE GENERALIZED NETWORK FORMULATION FOR APERTURE PROBLEMS-----	6
IV. THE SHORT-CIRCUIT FIELD DUE TO THE IMPRESSED SOURCES-----	11
V. THE PSEUDO-IMAGE METHOD OF OBTAINING THE SHORT-CIRCUIT FIELDS DUE TO THE MAGNETIC CURRENT EXPANSION FUNCTION-----	14
VI. EVALUATION OF THE ELECTRIC CURRENT COEFFICIENTS I_j^{inc} and I_j^a FOR TM PLANE WAVE EXCITATION-----	21
VII. EVALUATION OF THE MAGNETIC CURRENT COEFFICIENT V FOR TM PLANE WAVE EXCITATION-----	28
VIII. NUMERICAL RESULTS FOR A SLOTTED TM CIRCULAR CYLINDRICAL SURFACE-----	36
APPENDIX A. THE METHOD OF SOLUTION WITHOUT PSEUDO-IMAGE-----	42
APPENDIX B. THE FOURIER SERIES METHOD OF SOLUTION FOR A SLOTTED TM CIRCULAR CYLINDRICAL SURFACE-----	47
REFERENCES-----	53



Accession For	
NTIS CRA&I	<input checked="" type="checkbox"/>
DTIC TAB	<input type="checkbox"/>
Unannounced	<input type="checkbox"/>
Justification	
By	
Distribution /	
Availability Codes	
Dist	Avail and/or Special
A-1	

I. INTRODUCTION

The problem of electromagnetic scattering from a perfectly conducting surface S has been solved by first placing an unknown electric current \underline{J} on this surface, next writing the electric field integral equation for \underline{J} , and finally numerically solving this equation by the method of moments [1], [2]. The solution thus obtained will be accurate if S encloses neither a resonant cavity nor a cavity with an extremely small aperture, and if the maximum dimension of S is not more than a few wavelengths. The surface S may be two-dimensional or three-dimensional. Of course, if S is two-dimensional, then it is infinitely long in one direction, and we require only that its contour in the plane transverse to this direction be not more than a few wavelengths long.

If S forms a cavity with a very small aperture, then the above method will fail to accurately determine the field inside this cavity because this field, being the sum of the incident field and the field due to \underline{J} , will be very small. The field due to \underline{J} nearly cancels the incident field. Thus, a small percentage error in \underline{J} will give rise to a large percentage error in the field inside the cavity.

The field inside a cavity with a small aperture has been accurately determined by expressing it as the sum of the short-circuit field and the field due to an electric current source which is the negative of the short-circuit current on the shorted aperture [3]. This electric current source radiates in the presence of the conducting surface S . The short-circuit field is the field that would exist if the aperture were closed by a perfect conductor. The short-circuit current is the electric current that would exist on S if the aperture were closed by a perfect conductor.

An alternative method called the generalized network formulation for aperture problems [4]-[6] has been proposed for the case in which S forms a cavity with a small aperture. In this method, the aperture is closed with a perfect conductor, a sheet of unknown magnetic current \underline{M} is placed on one side of the shorted aperture, and $-\underline{M}$ is placed on the other side. The resulting situation will be the same as that of the original scattering problem if the component of magnetic field tangent to the shorted aperture is continuous across the shorted aperture. Following the method of moments, a linear combination of expansion functions is substituted for \underline{M} into the equation that expresses continuity of the tangential magnetic field across the shorted aperture and then this equation is solved numerically for the coefficients of the expansion functions. The generalized network formulation for aperture problems is easily implemented for an aperture in an infinite conducting plane because the electric current induced on the complete conducting plane by each expansion function for \underline{M} can be accounted for by imaging that expansion function about the plane [5], [6]. The complete conducting plane is the plane with the aperture shorted.

When the aperture is in a curved surface, the generalized network formulation for aperture problems is not as easy to implement because it is difficult to obtain the electromagnetic field produced by each expansion function for \underline{M} placed on either side of the shorted aperture and radiating in the presence of the complete conducting surface. The complete conducting surface is the conducting surface S with its aperture shorted. The problem of obtaining the electromagnetic field due to such an expansion function so radiating is a scattering problem in which the impressed source is on the scatterer. Two static problems of this type were con-

sidered in [7]. In the first problem, the objective was to find the electrostatic field due to an electrostatic dipole on the conducting surface of a sphere. The dipole was normal to the sphere. In the second problem, the objective was to find the magnetostatic field due to a magnetostatic dipole tangentially placed on the conducting surface of a sphere. In [7], each of these two static scattering problems was solved by a method in which a pseudo-image was used. We call this method the pseudo-image method.

The problem of electromagnetic scattering from an infinitely long, infinitesimally thin, perfectly conducting cylindrical surface with an infinitely long but narrow slot is stated in Section II. Solution by means of the generalized network formulation for aperture problems is outlined in Section III. In Sections II and III, the electromagnetic excitation is from impressed sources. The field due to the impressed sources radiating in the presence of the complete conducting surface is called the short-circuit field due to the impressed sources. This field is evaluated in Section IV. Only one expansion function for \underline{M} was used in Section III. In Section V, the pseudo-image method is used to obtain the short-circuit field due to this expansion function placed on either side of the shorted aperture. In Section VI, coefficients appearing in previously derived expressions for the short-circuit fields due to the impressed sources and to the expansion function for \underline{M} are evaluated for TM plane wave excitation. In Section VII, the coefficient of the expansion function for \underline{M} is evaluated for TM plane wave excitation.

II. STATEMENT OF THE PROBLEM

The combination of a known impressed electric current source \underline{J}^{imp} and a known impressed magnetic current source \underline{M}^{imp} radiates in a homogeneous medium with permeability μ and permittivity ϵ to produce an incident electromagnetic field $(\underline{E}^{inc}, \underline{H}^{inc})$ that is independent of z . An infinitely long perfectly conducting cylindrical surface called S is now placed in the medium. The axis of S is the z axis so that the electromagnetic field radiated by $(\underline{J}^{imp}, \underline{M}^{imp})$ in the presence of S is independent of z . This field is called $(\underline{E}, \underline{H})$.

Our purpose is to determine $(\underline{E}, \underline{H})$ when S is infinitely thin and, as viewed in the xy plane, appears as the contour shown in Fig. 1. This contour is a chain of $N-1$ straight line segments. The j th segment extends from the point P_j to the point P_{j+1} . The (x,y) coordinates of the points P_1 and P_N are $(0,w)$ and $(0,-w)$, respectively. The plane strip of area whose projection on the xy plane is the straight line segment between points P_N and P_1 in Fig. 1 is called the aperture. If there were no gap between the points P_N and P_1 , then S would enclose a cavity. If the gap were small, the straightforward method via solution of the electric field integral equation for the induced electric current on S would fail to accurately determine $(\underline{E}, \underline{H})$ inside the cavity. This method would fail because it gives $(\underline{E}, \underline{H})$ as the sum of two fields that nearly cancel each other inside the cavity, $(\underline{E}^{inc}, \underline{H}^{inc})$ and the field due to the induced electric current on S . The method of solution described in the next section accurately determines $(\underline{E}, \underline{H})$ when the gap is small.

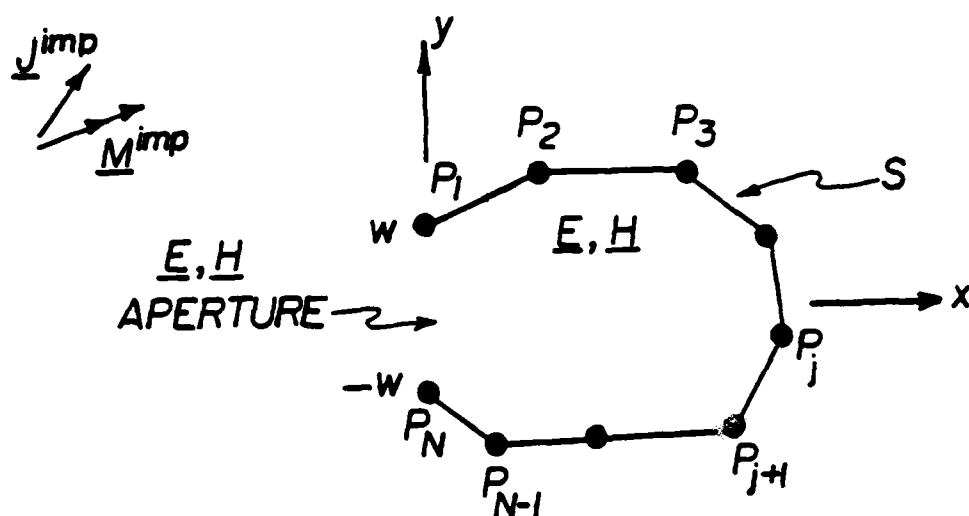


Fig. 1. The original problem as viewed in the xy plane. The two-dimensional sources \underline{J}^{imp} and \underline{M}^{imp} radiate in the presence of the cylindrical surface S .

III. SOLUTION BY THE GENERALIZED NETWORK FORMULATION FOR APERTURE PROBLEMS

The original problem of Fig. 1 is replaced by the equivalent problem of Fig. 2. The situation of Fig. 2 was obtained by closing the aperture with a perfectly conducting plane strip, placing the magnetic current sheet \underline{M} on the left-hand side of the strip, and placing $-\underline{M}$ on the right-hand side of the strip. Here,

$$\underline{M} = \underline{u}_x \times \underline{E} \quad (1)$$

where \underline{u}_x is the unit vector in the x direction and \underline{E} is the electric field in the aperture in Fig. 1. The combination of S and the plane strip that short circuits the aperture is called S^{sc} in Fig. 2. The surface S^{sc} divides space into two regions, an external region called region a and an interior or cavity region called region b.

If there was no electric current on the shorting strip in Fig. 2, then this strip could be removed. After removal of the shorting strip, the magnetic current sheets \underline{M} and $-\underline{M}$ would cancel each other resulting in the situation of Fig. 1. Therefore, the situation of Fig. 2 will be equivalent to that of Fig. 1 if there is no electric current on the shorting strip in Fig. 2. There will be no electric current on this shorting strip if the tangential magnetic field immediately to the left of the shorting strip is equal to the tangential magnetic field immediately to the right of the shorting strip. Hence, we write

$$\underline{H}_{\tan}^a(\underline{J}^{imp}, \underline{M}^{imp}) + \underline{H}_{\tan}^a(0, \underline{M}) = \underline{H}_{\tan}^b(0, -\underline{M}) \quad \text{on } A \quad (2)$$

where A is the surface of the shorting strip. The subscript tan in (2) denotes the component tangent to A. In (2), $\underline{H}_{\tan}^a(\underline{J}^{imp}, \underline{M}^{imp})$ is the magnetic

field in region a due to $(\underline{J}^{\text{imp}}, \underline{M}^{\text{imp}})$ radiating in the presence of S^{sc} , $\underline{H}^a(0, \underline{M})$ is the magnetic field in region a due to \underline{M} placed on the left-hand side of the shorting strip and radiating in the presence of S^{sc} , and $\underline{H}^b(0, -\underline{M})$ is the magnetic field in region b due to $-\underline{M}$ placed on the right-hand side of the shorting strip and radiating in the presence of S^{sc} . Each magnetic field in (2) has two arguments. The first argument is an electric current, and the second argument is a magnetic current. Actually, the left-hand side of (2) should be evaluated not exactly on A, but immediately to the left of A in region a. Moreover, the right-hand side of (2) should be evaluated not exactly on A, but immediately to the right of A in region b. Equation (2) ensures that the situation of Fig. 2 is equivalent to that of Fig. 1.

Since the situation of Fig. 2 is equivalent to that of Fig. 1, the electromagnetic field in Fig. 2 is equal to the unknown electromagnetic field $(\underline{E}, \underline{H})$ in Fig. 1. The field $(\underline{E}, \underline{H})$ in Fig. 2 is partitioned into $(\underline{E}^a, \underline{H}^a)$ and $(\underline{E}^b, \underline{H}^b)$ where $(\underline{E}^a, \underline{H}^a)$ is the field in region a, and $(\underline{E}^b, \underline{H}^b)$ is the field in region b.

$$(\underline{E}, \underline{H}) = \begin{cases} (\underline{E}^a, \underline{H}^a), & \text{region a} \\ (\underline{E}^b, \underline{H}^b), & \text{region b} \end{cases} \quad (3)$$

$$\underline{E}^a = \underline{E}^a(\underline{J}^{\text{imp}}, \underline{M}^{\text{imp}}) + \underline{E}^a(0, \underline{M}) \quad (4)$$

$$\underline{H}^a = \underline{H}^a(\underline{J}^{\text{imp}}, \underline{M}^{\text{imp}}) + \underline{H}^a(0, \underline{M}) \quad (5)$$

$$\underline{E}^b = \underline{E}^b(0, -\underline{M}) \quad (6)$$

$$\underline{H}^b = \underline{H}^b(0, -\underline{M}) \quad (7)$$

The magnetic fields on the right-hand sides of (5) and (7) were defined in the previous paragraph. The \underline{E} 's on the right-hand sides of (4) and (6) are the corresponding electric fields. Namely, $\underline{E}^a(\underline{J}^{imp}, \underline{M}^{imp})$ is the electric field in region a due to $(\underline{J}^{imp}, \underline{M}^{imp})$ radiating in the presence of S^{sc} , $\underline{E}^a(0, \underline{M})$ is the electric field in region a due to \underline{M} placed on the left-hand side of the shorting strip and radiating in the presence of S^{sc} , and $\underline{E}^b(0, -\underline{M})$ is the electric field in region b due to $-\underline{M}$ placed on the right-hand side of the shorting strip and radiating in the presence of S^{sc} . Each electric field on the right-hand sides of (4) and (6) has two arguments. The first argument is an electric current, and the second argument is a magnetic current.

Some fields on the right-hand sides of (4)-(7) depend on \underline{M} . To determine \underline{M} , we appeal to (2). Rearranging the terms in (2), we obtain

$$-\underline{H}_{tan}^a(0, \underline{M}) - \underline{H}_{tan}^b(0, \underline{M}) = \underline{H}_{tan}^a(\underline{J}^{imp}, \underline{M}^{imp}) \quad \text{on } A \quad (8)$$

Next, \underline{M} is approximated by

$$\underline{M} = V \underline{M}_1 \quad (9)$$

where V is an unknown complex constant to be evaluated later and \underline{M}_1 is an expansion function that will be specified later when the incident field $(\underline{E}^{inc}, \underline{H}^{inc})$ is specialized to a TM field. The expansion function \underline{M}_1 will be tangent to S^{sc} and independent of z where z is the coordinate measured perpendicular to the xy plane. The magnetic fields in (8) will also be independent of z so that it will suffice to satisfy (8) only on the projection of A in the xy plane. This projection is the straight line segment between the points P_N and P_1 in Fig. 2. Substituting (9) into (8), taking the scalar product of (8) with \underline{M}_1 , and then integrating this product

from $-w$ to w with respect to y at $x=0$, we obtain

$$(Y^a + Y^b)V = I \quad (10)$$

where

$$Y^a = - \int_{-w}^w \underline{M}_1 \cdot \underline{H}^a(0, \underline{M}_1) dy \quad (11)$$

$$Y^b = - \int_{-w}^w \underline{M}_1 \cdot \underline{H}^b(0, \underline{M}_1) dy \quad (12)$$

$$I = \int_{-w}^w \underline{M}_1 \cdot \underline{H}^a(\underline{J}^{imp}, \underline{M}^{imp}) dy \quad (13)$$

Actually, the magnetic fields in (11) and (13) are evaluated not exactly at $x=0$ on the shorting strip, but immediately to the left of the shorting strip in region a. Moreover, the magnetic field in (12) is evaluated not exactly at $x=0$ on the shorting strip, but immediately to the right of the shorting strip in region b.

If Y^a , Y^b , and I can be determined, then (10) can be solved for V . Substitution of (9) into (4)-(7) gives

$$\underline{E}^a = \underline{E}^a(\underline{J}^{imp}, \underline{M}^{imp}) + V \underline{E}^a(0, \underline{M}_1) \quad (14)$$

$$\underline{H}^a = \underline{H}^a(\underline{J}^{imp}, \underline{M}^{imp}) + V \underline{H}^a(0, \underline{M}_1) \quad (15)$$

$$\underline{E}^b = - V \underline{E}^b(0, \underline{M}_1) \quad (16)$$

$$\underline{H}^b = - V \underline{H}^b(0, \underline{M}_1) \quad (17)$$

The electromagnetic fields on the right-hand sides of (14)-(17) are obtained in the next two sections. The magnetic fields so obtained are then substituted into expressions (11)-(13) for Y^a , Y^b , and I .

IV. THE SHORT-CIRCUIT FIELD DUE TO THE IMPRESSED SOURCES

In this section, the electromagnetic field ($\underline{E}^a(\underline{J}^{imp}, \underline{M}^{imp})$, $\underline{H}^a(\underline{J}^{imp}, \underline{M}^{imp})$) which appears in (14) and (15) is evaluated. This field is the field in region a due to the impressed sources ($\underline{J}^{imp}, \underline{M}^{imp}$) radiating in the presence of S^{sc} . The xy plane view of the situation in which this field exists is shown in Fig. 3. It is evident from Fig. 3 that

$$\underline{E}^a(\underline{J}^{imp}, \underline{M}^{imp}) = \underline{E}^{inc} + \underline{E}(\underline{J}^{inc}, 0) \quad \text{in region a} \quad (18)$$

and

$$\underline{H}^a(\underline{J}^{imp}, \underline{M}^{imp}) = \underline{H}^{inc} + \underline{H}(\underline{J}^{inc}, 0) \quad \text{in region a} \quad (19)$$

where \underline{J}^{inc} is the electric current induced on S^{sc} by ($\underline{J}^{imp}, \underline{M}^{imp}$). In (18) and (19), ($\underline{E}^{inc}, \underline{H}^{inc}$) is the electromagnetic field due to ($\underline{J}^{imp}, \underline{M}^{imp}$) radiating in the presence of the homogeneous medium characterized by (μ, ϵ), and ($\underline{E}(\underline{J}^{inc}, 0), \underline{H}(\underline{J}^{inc}, 0)$) is the electromagnetic field due to the electric current \underline{J}^{inc} radiating in the presence of the same homogeneous medium. Although the right-hand sides of (18) and (19) are defined in all space, the left-hand sides of (18) and (19) are defined only in region a so that (18) and (19) can be valid only in region a.

Since S^{sc} is perfectly conducting in Fig. 3,

$$\underline{E}_{tan}^a(\underline{J}^{imp}, \underline{M}^{imp}) = 0 \quad \text{on } S^{sc} \quad (20)$$

where the subscript tan denotes the component tangent to S^{sc} . Because the field in (20) is given by (18), we obtain the following equation for \underline{J}^{inc} .

$$-\underline{E}_{tan}(\underline{J}^{inc}, 0) = \underline{E}_{tan}^{inc} \quad \text{on } S^{sc} \quad (21)$$

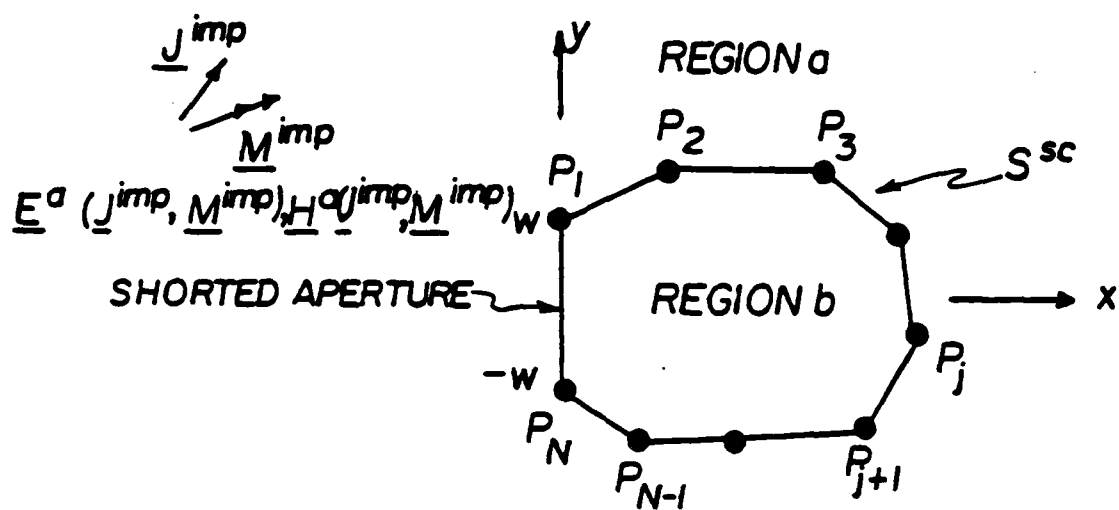


Fig. 3. The xy plane view of the situation in which the electromagnetic field $(\underline{E}^a(\underline{J}^{imp}, \underline{M}^{imp}), \underline{H}^a(\underline{J}^{imp}, \underline{M}^{imp}))$ exists.

The electric current \underline{J}^{inc} in (21) is approximated by

$$\underline{J}^{inc} = \sum_{j=1}^N I_j^{inc} \underline{J}_j \quad (22)$$

where $\{I_j^{inc}\}$ are unknown constants and $\{\underline{J}_j\}$ are expansion functions that will be specified later when the incident field $(\underline{E}^{inc}, \underline{H}^{inc})$ is specialized to a TM field. Each of the expansion functions $\{\underline{J}_j\}$ will be on S^{sc} , tangent to S^{sc} , and independent of z .

Equation (22) is substituted into (21) and then the scalar product of (21) with \underline{J}_i is integrated around the contour of S^{sc} in the xy plane. Letting $i = 1, 2, \dots, N$, we obtain N simultaneous equations which are written in matrix form as

$$Z \underline{I}^{inc} = \underline{V}^{inc} \quad (23)$$

where Z is a square matrix of order N and each of the quantities \underline{I}^{inc} and \underline{V}^{inc} is a column vector of N elements. The j th element of \underline{I}^{inc} is the constant I_j^{inc} that appears in (22). The ij th element of Z is called Z_{ij} and is given by

$$Z_{ij} = - \int_0^{t_{N+1}} \underline{J}_i \cdot \underline{E}(\underline{J}_j, 0) dt \quad (24)$$

where the variable of integration t is the arc length along the contour of S^{sc} in the xy plane. Starting from zero at the point P_1 in Fig. 3, the variable t increases as the contour is transversed in the clockwise direction, attaining the value t_{N+1} upon arrival back at the starting point P_1 . The i th element of \underline{V}^{inc} in (23) is called V_i^{inc} and is given by

$$V_i^{inc} = \int_0^{t_{N+1}} \underline{J}_i \cdot \underline{E}^{inc} dt \quad (25)$$

After the elements of Z and \vec{V}^{inc} have been obtained, (23) can be solved for \vec{I}^{inc} . The electric current \underline{J}^{inc} will then be given by (22) in which I_j^{inc} is the j th element of \vec{I}^{inc} . Substitution of (22) into (18) and (19) gives

$$\underline{E}^a(\underline{J}^{imp}, \underline{M}^{imp}) = \underline{E}^{inc} + \sum_{j=1}^N I_j^{inc} \underline{E}(\underline{J}_j, 0) \quad \text{in region a} \quad (26)$$

and

$$\underline{H}^a(\underline{J}^{imp}, \underline{M}^{imp}) = \underline{H}^{inc} + \sum_{j=1}^N I_j^{inc} \underline{H}(\underline{J}_j, 0) \quad \text{in region a} \quad (27)$$

Substituting (27) into (13), we obtain

$$I = \int_{-w}^w \underline{M}_1 \cdot \underline{H}^{inc} dy + \sum_{j=1}^N I_j^{inc} \int_{-w}^w \underline{M}_1 \cdot \underline{H}^-(\underline{J}_j, 0) dy \quad (28)$$

where the superscript "-" denotes magnetic field evaluation at $x=0^-$, that is, immediately to the left of the shorting strip.

V. THE PSEUDO-IMAGE METHOD OF OBTAINING THE SHORT-CIRCUIT FIELDS DUE TO THE MAGNETIC CURRENT EXPANSION FUNCTION

In this section, the electromagnetic fields ($\underline{E}^a(0, \underline{M}_1)$, $\underline{H}^a(0, \underline{M}_1)$) and ($\underline{E}^b(0, \underline{M}_1)$, $\underline{H}^b(0, \underline{M}_1)$) of (14)-(17) are evaluated by means of a method called the pseudo-image method. Here, $\underline{E}^a(0, \underline{M}_1)$ and $\underline{H}^a(0, \underline{M}_1)$ are, respectively, the electric and magnetic fields in region a due to the magnetic current sheet \underline{M}_1 placed on the left-hand side of the shorted aperture and radiating in the presence of S^{sc} . Moreover, $\underline{E}^b(0, \underline{M}_1)$ and $\underline{H}^b(0, \underline{M}_1)$ are, respectively, the electric and magnetic fields in region b due to the

magnetic current sheet \underline{M}_1 placed on the right-hand side of the shorted aperture and radiating in the presence of S^{sc} .

Figure 4 shows the xy plane view of the situation in which $(\underline{E}^a(0, \underline{M}_1), \underline{H}^a(0, \underline{M}_1))$ exists. Since the perfectly conducting surface S^{sc} completely isolates region b from region a, any source can be placed in region b without affecting the electromagnetic field $(\underline{E}^a(0, \underline{M}_1), \underline{H}^a(0, \underline{M}_1))$ in region a. We place the magnetic current sheet \underline{M}_1 on the right-hand side of the shorted aperture as shown in Fig. 5.

The field in region a of Fig. 5 is the same as that in region a of Fig. 4, namely, $(\underline{E}^a(0, \underline{M}_1), \underline{H}^a(0, \underline{M}_1))$. The magnetic current sheet on the right-hand side of the shorted aperture in Fig. 5 is called the pseudo-image of the magnetic current sheet on the left-hand side of the shorted aperture. The pseudo-image annihilates the primary electric field excitation on the shorted aperture. This annihilation should considerably reduce the electric current induced on S^{sc} and, hopefully, improve the behavior of this current so that it can be more accurately approximated by a linear combination of simple expansion functions.

It is evident from Fig. 5 that

$$\underline{E}^a(0, \underline{M}_1) = \underline{E}(0, 2\underline{M}_1) + \underline{E}(\underline{J}^a, 0) \quad \text{in region a} \quad (29)$$

and

$$\underline{H}^a(0, \underline{M}_1) = \underline{H}(0, 2\underline{M}_1) + \underline{H}(\underline{J}^a, 0) \quad \text{in region a} \quad (30)$$

where \underline{J}^a is the electric current induced on S^{sc} in Fig. 5, and $2\underline{M}_1$ represents the combination of the two magnetic current sheets in Fig. 5, each of density \underline{M}_1 . On the right-hand sides of (29) and (30), $(\underline{E}(\underline{J}^a, 0), \underline{H}(\underline{J}^a, 0))$ is the electromagnetic field due to the electric current \underline{J}^a , and $(\underline{E}(0, 2\underline{M}_1),$

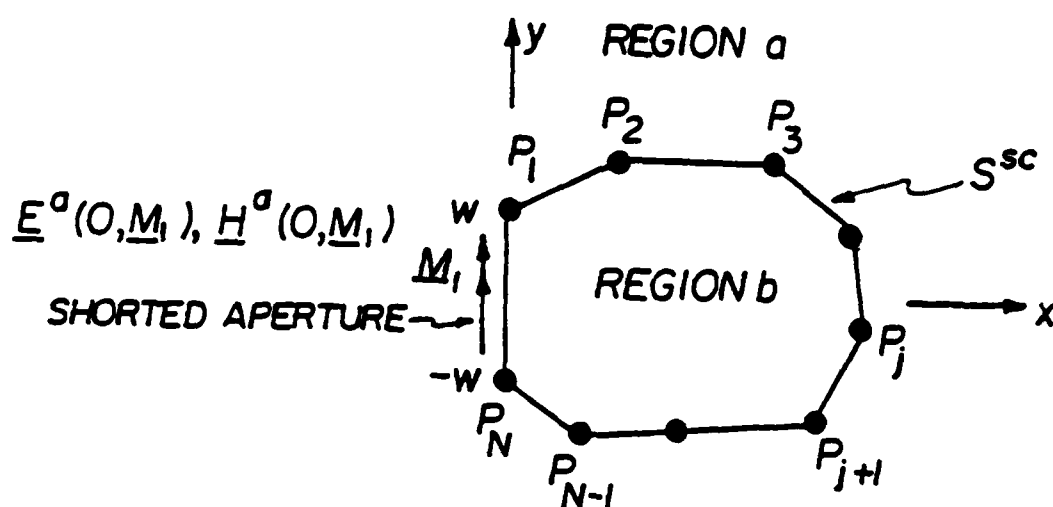


Fig. 4. The xy plane view of the situation in which the electromagnetic field $(\underline{E}^a(0, \underline{M}_1), \underline{H}^a(0, \underline{M}_1))$ exists.

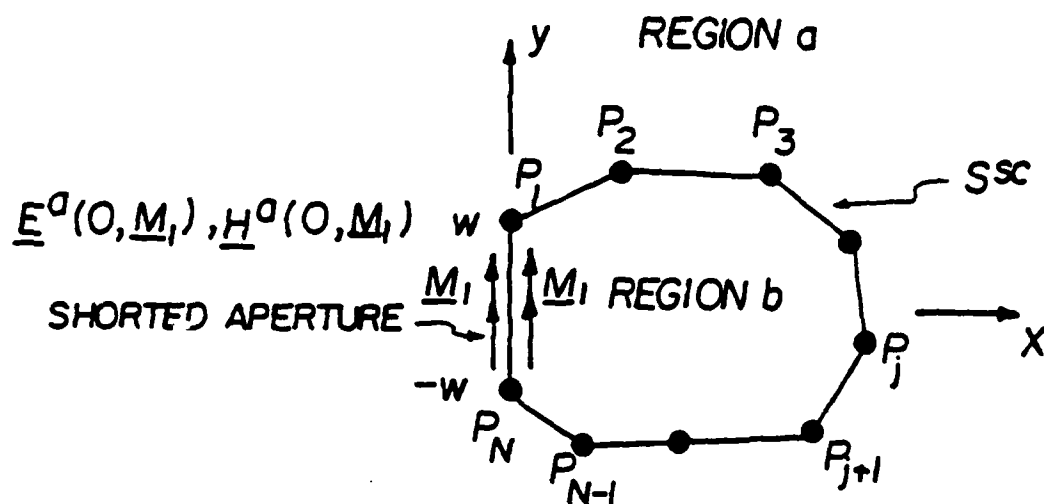


Fig. 5. The xy plane view of the equivalent situation in which the electromagnetic field $(\underline{E}^a(0, \underline{M}_1), \underline{H}^a(0, \underline{M}_1))$ exists. The magnetic current sheet immediately to the right of the shorted aperture is called the pseudo-image of the one immediately to the left.

$\underline{H}(0, 2\underline{M}_1)$ is the electromagnetic field due to the magnetic current $2\underline{M}_1$. In the previous sentence, both \underline{J}^a and $2\underline{M}_1$ radiate in the presence of the homogeneous medium characterized by (μ, ϵ) . The right-hand sides of (29) and (30) are the fields everywhere in Fig. 5, whereas the left-hand sides of (29) and (30) are defined only in region a so that (29) and (30) can be valid only in region a.

In order to determine $\underline{E}^a(0, \underline{M}_1)$ and $\underline{H}^a(0, \underline{M}_1)$, we must, according to (29) and (30), first determine \underline{J}^a . Since S^{sc} is perfectly conducting in Fig. 5,

$$\underline{E}_{\tan}^a(0, \underline{M}_1) = 0 \quad \text{on } S^{sc} \quad (31)$$

where the subscript tan denotes the component tangent to S^{sc} . Because the field in (31) is given by (29), we obtain the following equation for \underline{J}^a .

$$-\underline{E}_{\tan}(\underline{J}^a, 0) = \underline{E}_{\tan}(0, 2\underline{M}_1) \quad \text{on } S^{sc} \quad (32)$$

When $\underline{E}_{\tan}(0, 2\underline{M}_1)$ is evaluated on the part of S^{sc} labeled the shorted aperture in Fig. 5, the magnetic current $2\underline{M}_1$ is split into two current sheets, each of density \underline{M}_1 , one on each side of the shorted aperture. As a result, $\underline{E}_{\tan}(0, 2\underline{M}_1)$ vanishes on the shorted aperture. When $\underline{E}_{\tan}(0, 2\underline{M}_1)$ is evaluated on the remaining part of S^{sc} , $2\underline{M}_1$ is taken to be a single sheet of magnetic current of density $2\underline{M}_1$ on the shorted aperture.

The electric current \underline{J}^a in (32) is approximated by

$$\underline{J}^a = \sum_{j=1}^N I_j^a \underline{J}_j \quad (33)$$

where $\{I_j^a\}$ are unknown constants and $\{\underline{J}_j\}$ are the expansion functions that appear in (22). Expression (33) is substituted into (32) and then the scalar product of (32) with \underline{J}_i is integrated around the contour of S^{sc} in

the xy plane. Letting $i = 1, 2, \dots, N$, we obtain N simultaneous equations which can be written in matrix form as

$$Z \vec{I}^a = \vec{V}^a \quad (34)$$

where Z is the $N \times N$ matrix that appears in (23) and each of the quantities \vec{I}^a and \vec{V}^a is a column vector of N elements. The j th element of \vec{I}^a is the constant I_j^a that appears in (33). The i th element of \vec{V}^a is called V_i^a and is given by

$$V_i^a = \int_0^{t_{N+1}} \underline{J}_i \cdot \underline{E}(0, 2\underline{M}_1) dt \quad (35)$$

where t and t_{N+1} are the same as in (25).

After the elements of Z and \vec{V}^a have been obtained, (34) can be solved for \vec{I}^a . The electric current \underline{J}^a will then be given by (33) in which I_j^a is the j th element of \vec{I}^a . Substitution of (33) into (29) and (30) gives

$$\underline{E}^a(0, \underline{M}_1) = \underline{E}(0, 2\underline{M}_1) + \sum_{j=1}^N I_j^a \underline{E}(\underline{J}_j, 0) \quad \text{in region a} \quad (36)$$

and

$$\underline{H}^a(0, \underline{M}_1) = \underline{H}(0, 2\underline{M}_1) + \sum_{j=1}^N I_j^a \underline{H}(\underline{J}_j, 0) \quad \text{in region a} \quad (37)$$

The right-hand sides of (36) and (37) are the fields everywhere in Fig. 5, whereas the left-hand sides of (36) and (37) are defined only in region a so that (36) and (37) can be valid only in region a. Substituting (37) into (11), we obtain

$$Y^a = - \int_{-w}^w \underline{M}_1 \cdot \underline{H}(0, 2\underline{M}_1) dy - \sum_{j=1}^N I_j^a \int_{-w}^w \underline{M}_1 \cdot \underline{H}^-(\underline{J}_j, 0) dy \quad (38)$$

where the superscript "-" denotes magnetic field evaluation at $x=0^-$, that is,

immediately to the left of the shorting strip.

In (16) and (17), $(\underline{E}^b(0, \underline{M}_1), \underline{H}^b(0, \underline{M}_1))$ is the electromagnetic field in region b due to the magnetic current sheet \underline{M}_1 placed on the right-hand side of the shorted aperture and radiating in the presence of S^{sc} . Since the perfectly conducting surface S^{sc} completely isolates region a from region b, the magnetic current sheet \underline{M}_1 can be placed on the left-hand side of the shorting strip without affecting the electromagnetic field $(\underline{E}^b(0, \underline{M}_1), \underline{H}^b(0, \underline{M}_1))$ in region b. Introduction of this current sheet gives the situation of Fig. 5. Since the electromagnetic field everywhere in Fig. 5 is given by the right-hand sides of (36) and (37), it is evident that

$$\underline{E}^b(0, \underline{M}_1) = \underline{E}(0, 2\underline{M}_1) + \sum_{j=1}^N I_j^a \underline{E}(\underline{J}_j, 0) \quad \text{in region b} \quad (39)$$

and

$$\underline{H}^b(0, \underline{M}_1) = \underline{H}(0, 2\underline{M}_1) + \sum_{j=1}^N I_j^a \underline{H}(\underline{J}_j, 0) \quad \text{in region b} \quad (40)$$

Substituting (40) into (12), we obtain

$$Y^b = - \int_{-w}^w \underline{M}_1 \cdot \underline{H}(0, 2\underline{M}_1) dy - \sum_{j=1}^N I_j^a \int_{-w}^w \underline{M}_1 \cdot \underline{H}^+(\underline{J}_j, 0) dy \quad (41)$$

where the superscript "+" denotes magnetic field evaluation at $x=0^+$, that is, immediately to the right of the shorting strip.

The electromagnetic field $(\underline{E}, \underline{H})$ of Fig. 1 is now given by (3) in which \underline{E}^a is obtained by substituting (26) and (36) into (14), \underline{H}^a is obtained by substituting (27) and (37) into (15), \underline{E}^b is obtained by substituting (39) into (16), and \underline{H}^b is obtained by substituting (40) into (17).

$$\underline{E} = \begin{cases} (\underline{E}^{inc} + \sum_{j=1}^N I_j^{inc} \underline{E}(\underline{J}_j, 0)) + V(\underline{E}(0, 2\underline{M}_1) + \sum_{j=1}^N I_j^a \underline{E}(\underline{J}_j, 0)), & \text{region a} \\ -V(\underline{E}(0, 2\underline{M}_1) + \sum_{j=1}^N I_j^a \underline{E}(\underline{J}_j, 0)) & , \text{region b} \end{cases} \quad (42)$$

$$\underline{H} = \begin{cases} (\underline{H}^{inc} + \sum_{j=1}^N I_j^{inc} \underline{H}(\underline{J}_j, 0)) + V(\underline{H}(0, 2\underline{M}_1) + \sum_{j=1}^N I_j^a \underline{H}(\underline{J}_j, 0)), & \text{region a} \\ -V(\underline{H}(0, 2\underline{M}_1) + \sum_{j=1}^N I_j^a \underline{H}(\underline{J}_j, 0)) & , \text{region b} \end{cases} \quad (43)$$

In (42) and (43), I_j^{inc} is the j th element of the column vector \vec{I}^{inc} that satisfies (23) in which the ij th element of Z is given by (24) and the i th element of \vec{V}^{inc} is given by (25). Furthermore, I_j^a is the j th element of the column vector \vec{I}^a that satisfies (34) in which the ij th element of Z is given by (24) and the i th element of \vec{V}^a is given by (35). Moreover, V is the complex number that satisfies (10) in which Y^a , Y^b , and I are given by (38), (41), and (28), respectively.

VI. EVALUATION OF THE ELECTRIC CURRENT COEFFICIENTS I_j^{inc} AND I_j^a FOR TM PLANE WAVE EXCITATION

In this section, the coefficients $\{I_j^{inc}\}$ and $\{I_j^a\}$ that appear in (42) and (43) are evaluated for the case in which the incident electromagnetic field $(\underline{E}^{inc}, \underline{H}^{inc})$ is the TM plane wave given by

$$\underline{E}^{inc} = \underline{u}_z e^{jk(x \cos \phi^{inc} + y \sin \phi^{inc})} \quad (44)$$

$$\underline{H}^{inc} = \frac{1}{\eta} (-\underline{u}_x \sin \phi^{inc} + \underline{u}_y \cos \phi^{inc}) e^{jk(x \cos \phi^{inc} + y \sin \phi^{inc})} \quad (45)$$

where \underline{u}_x , \underline{u}_y , and \underline{u}_z are the unit vectors in the x , y , and z directions,

respectively. Moreover, n and k are, respectively, the intrinsic impedance and wave number of the homogeneous medium with permeability μ and permittivity ϵ . Furthermore, ϕ^{inc} is the azimuthal angle of the direction from which the plane wave comes. Measured in the xy plane, ϕ^{inc} is zero on the positive x axis and increases as the y axis is approached.

When $(\underline{E}^{inc}, \underline{H}^{inc})$ is the TM field given by (44) and (45), we let the electric current expansion function \underline{J}_j be the z directed pulse of unit amplitude on the j th segment of the contour of S^{sc} in the xy plane.

$$\underline{J}_j(t) = \begin{cases} \underline{u}_z, & t_j \leq t < t_{j+1} \\ 0, & \text{otherwise} \end{cases}, \quad j=1,2,\dots,N \quad (46)$$

In (46), t_j is the value of t at the point P_j . The previous statement is valid for $j=1,2,\dots,N$. As in (24), t_{N+1} is the total length of the contour of S^{sc} in the xy plane. For $j=1,2,\dots,N-1$, the j th segment of the contour of S^{sc} in the xy plane is the straight line segment that runs from the point P_j to the point P_{j+1} in Fig. 3. The N th segment of the contour of S^{sc} in the xy plane is the straight line segment that runs from the point P_N to the point P_1 in Fig. 3.

When $(\underline{E}^{inc}, \underline{H}^{inc})$ is the TM field given by (44) and (45), we let the magnetic current expansion function \underline{M}_1 be the function of y given by

$$\underline{M}_1(y) = \begin{cases} \underline{u}_y \sqrt{1 - (y/w)^2}, & -w \leq y \leq w \\ 0, & |y| > w \end{cases} \quad (47)$$

To solve (23) for \vec{I}^{inc} , we must first evaluate the elements of Z and \vec{V}^{inc} . The electric field $\underline{E}(\underline{J}_j, 0)$ that appears in expression (24) for Z_{ij} is given by [8, eq. (3-5)]

$$\underline{E}(\underline{J}_j, 0) = - \frac{k\eta}{4} \int_0^{t_{N+1}} \underline{J}_j(t') H_0^{(2)}(k\sqrt{(x-x')^2 + (y-y')^2}) dt' \quad (48)$$

where $H_0^{(2)}$ is the Hankel function of the second kind of order zero. Furthermore, (x, y) are the rectangular coordinates of the point at which $\underline{E}(\underline{J}_j, 0)$ is evaluated, and (x', y') are the rectangular coordinates of the point on the contour of S^{sc} at which the arc length is t' . In view of (46), substitution of (48) into (24) gives

$$Z_{ij} = \frac{k\eta}{4} \int_{t_i}^{t_{i+1}} dt \int_{t_j}^{t_{j+1}} dt' H_0^{(2)}(k\sqrt{(x-x')^2 + (y-y')^2}) \quad (49)$$

where (x, y) are the rectangular coordinates of the point on the contour of S^{sc} at which the arc length is t .

If new variables of integration u and u' are defined by

$$u = k(t - 0.5(t_i + t_{i+1})) \quad (50)$$

and

$$u' = k(t' - 0.5(t_j + t_{j+1})) \quad (51)$$

then (49) becomes

$$Z_{ij} = \frac{\eta}{4k} \int_{-0.5\gamma_i}^{0.5\gamma_i} du \int_{-0.5\gamma_j}^{0.5\gamma_j} du' H_0^{(2)}(\alpha_{ij}) \quad (52)$$

In (52),

$$\gamma_i = k\sqrt{(x_{i+1} - x_i)^2 + (y_{i+1} - y_i)^2} \quad (53)$$

where (x_i, y_i) are the (x, y) coordinates of the point on the contour of S^{sc} at which the arc length is t_i . Furthermore,

$$\alpha_{ij} = \sqrt{(kx_i^+ - kx_j^+ + u \cos \phi_i - u' \cos \phi_j)^2 + (ky_i^+ - ky_j^+ + u \sin \phi_i - u' \sin \phi_j)^2} \quad (54)$$

where x_i^+ and y_i^+ are, respectively, the x and y coordinates of the midpoint of the i th segment of the contour of S^{sc} , and ϕ_i is the angle that the i th segment makes with the positive x axis. More precisely,

$$x_i^+ = 0.5(x_{i+1} + x_i) \quad (55)$$

$$y_i^+ = 0.5(y_{i+1} + y_i) \quad (56)$$

$$\cos \phi_i = \frac{k(x_{i+1} - x_i)}{\gamma_i} \quad (57)$$

$$\sin \phi_i = \frac{k(y_{i+1} - y_i)}{\gamma_i} \quad (58)$$

If $i \neq j$, the double integral in (52) is evaluated by the method of two-dimensional Gaussian quadrature. If $i = j$, (52) reduces to

$$Z_{ii} = \frac{n}{4k} \int_{-0.5\gamma_i}^{0.5\gamma_i} du \int_{-0.5\gamma_i}^{0.5\gamma_i} du' H_0^{(2)}(|u-u'|) \quad (59)$$

The bracketed term on the right-hand side of the identity

$$H_0^{(2)}(x) = 1 - \frac{j2}{\pi} \ln \left(\frac{\gamma x}{2} \right) + [H_0^{(2)}(x) - 1 + \frac{j2}{\pi} \ln \left(\frac{\gamma x}{2} \right)] \quad (60)$$

approaches zero as x approaches zero [9, p. 462]. Here, $\ln \gamma$ is Euler's constant. Substitution of (60) into (59) gives

$$Z_{ii} = \frac{n}{4k} \left\{ C + \int_{-0.5\gamma_i}^{0.5\gamma_i} du \int_{-0.5\gamma_i}^{0.5\gamma_i} du' [H_0^{(2)}(|u-u'|) - 1 + \frac{j2}{\pi} \ln \left(\frac{\gamma |u-u'|}{2} \right)] \right\} \quad (61)$$

where

$$C = \int_{-0.5\gamma_1}^{0.5\gamma_1} du \int_{-0.5\gamma_1}^{0.5\gamma_1} du' \left[1 - \frac{j2}{\pi} \ln \left(\frac{\gamma|u-u'|}{2} \right) \right] \quad (62)$$

Using [10, Formulas 610. and 610.1.] to evaluate the double integral in (62), we obtain

$$C = \gamma_1^2 + \frac{j\gamma_1^2}{\pi} \left(3 - 2 \ln \left(\frac{\gamma\gamma_1}{2} \right) \right) \quad (63)$$

Substitution of (63) into (61) gives

$$Z_{ii} = \frac{\eta}{4k} \left\{ \gamma_1^2 + \frac{j\gamma_1^2}{\pi} \left(3 - 2 \ln \left(\frac{\gamma\gamma_1}{2} \right) \right) + \int_{-0.5\gamma_1}^{0.5\gamma_1} du \int_{-0.5\gamma_1}^{0.5\gamma_1} du' \left[H_0^{(2)}(|u-u'|) - 1 + \frac{j2}{\pi} \ln \left(\frac{\gamma|u-u'|}{2} \right) \right] \right\} \quad (64)$$

Since its integrand is bounded, the iterated integral in (64) can be accurately evaluated by the method of two-dimensional Gaussian quadrature.

Substituting (44) and (46) into (25), we obtain

$$v_i^{inc} = \int_{t_i}^{t_{i+1}} e^{jk(x \cos \phi^{inc} + y \sin \phi^{inc})} dt \quad (65)$$

where (x,y) are the rectangular coordinates of the point on the contour of S^{sc} at which the arc length is t. If the variable of integration in (65) is changed from t to u of (50), then (65) becomes

$$v_i^{inc} = \frac{1}{k} e^{jk(x_i^+ \cos \phi^{inc} + y_i^+ \sin \phi^{inc})} \int_{-0.5\gamma_1}^{0.5\gamma_1} e^{ju \cos(\phi_i - \phi^{inc})} du \quad (66)$$

The integral in (66) being tractable, (66) reduces to

$$V_i^{inc} = \frac{\gamma_i}{k} e^{jk(x_i^+ \cos \phi^{inc} + y_i^+ \sin \phi^{inc})} \frac{\sin(0.5\gamma_i \cos(\phi_i - \phi^{inc}))}{0.5\gamma_i \cos(\phi_i - \phi^{inc})} \quad (67)$$

Now, the quantities Z and \vec{V}^{inc} that appear in (23) are known, the diagonal elements of Z being given by (64), the remaining elements of Z by (52), and the elements of \vec{V}^{inc} by (67). Next, (23) is solved for \vec{I}^{inc} . The coefficients $\{I_j^{inc}\}$ will then be the elements of \vec{I}^{inc} .

To solve (34) for \vec{I}^a , we must first evaluate the elements of \vec{V}^a . In the $\underline{E}(0, 2\underline{M}_1)$ that appears in (35), $2\underline{M}_1$ represents the two magnetic currents, each of density \underline{M}_1 , that straddle the y axis in Fig. 5. Therefore, $\underline{E}(0, 2\underline{M}_1)$ vanishes on the y axis. Because \underline{J}_N is on the y axis and because $\underline{E}(0, 2\underline{M}_1)$ vanishes there, it is evident from (35) that

$$V_N^a = 0 \quad (68)$$

The next two paragraphs are devoted to evaluating V_i^a for $i \neq N$.

The electric field $\underline{E}(0, 2\underline{M}_1)$ that appears in expression (35) for V_i^a is given by [9, eqs. (3-4) and (5-96)]

$$\underline{E}(0, 2\underline{M}_1) = \frac{1}{2} \nabla \times \int_{-w}^w \underline{M}_1(y') H_0^{(2)}(k \sqrt{x^2 + (y-y')^2}) dy' \quad (69)$$

where (x,y) are the rectangular coordinates of the point at which $\underline{E}(0, 2\underline{M}_1)$ is evaluated. Furthermore, " $\nabla \times$ " is the curl operator with respect to the coordinates (x,y) . If $i \neq N$, then \underline{J}_i is remote from the magnetic current sheet $2\underline{M}_1$ so that the $\underline{E}(0, 2\underline{M}_1)$ that appears in (35) is not evaluated on this magnetic current sheet. In this case, the curl operator in (69) can be taken under the integral sign. Taking the curl operator under the integral sign, substituting (47) for \underline{M}_1 in (69), and using [9, eqs. (A-14) and (D-15)], we obtain

$$\underline{E}(0, 2\underline{M}_1) = -\underline{u}_z \frac{jkx}{2} \int_{-w}^w \frac{\sqrt{1 - (y'/w)^2} H_1^{(2)}(k\sqrt{x^2 + (y-y')^2})}{\sqrt{x^2 + (y-y')^2}} dy' \quad (70)$$

Substitution of (70) and (46) into (35) gives

$$V_i^a = -\frac{jk}{2} \int_{t_i}^{t_{i+1}} dt \int_{-w}^w dy' \frac{x\sqrt{1 - (y'/w)^2} H_1^{(2)}(k\sqrt{x^2 + (y-y')^2})}{\sqrt{x^2 + (y-y')^2}}, \quad i=1,2,\dots,N-1 \quad (71)$$

where (x,y) are the rectangular coordinates of the point on the contour of S^{sc} at which the arc length is t . If new variables of integration u and u' are defined by

$$u = k(t - 0.5 (t_i + t_{i+1})) \quad (72)$$

and

$$u' = ky' \quad (73)$$

then (71) becomes

$$V_i^a = -\frac{j}{2k} \int_{-0.5\gamma_i}^{0.5\gamma_i} du (kx_i^+ + u \cos \phi_i) \int_{-kw}^{kw} du' \frac{\sqrt{1 - (\frac{u'}{kw})^2} H_1^{(2)}(\alpha_{iN})}{\alpha_{iN}}, \quad i=1,2,\dots,N-1 \quad (74)$$

where γ_i , x_i^+ , $\cos \phi_i$, and α_{iN} are given by (53), (55), (57), and (54), respectively. Because of the orientation of the N th segment of the contour of S^{sc} , expression (54) for α_{iN} reduces to

$$\alpha_{iN} = \sqrt{(kx_i^+ + u \cos \phi_i)^2 + (ky_i^+ + u \sin \phi_i - u')^2} \quad (75)$$

The double integral in (74) is evaluated by the method of two-dimensional Gaussian quadrature. Now, the quantities Z and \vec{V}^a that appear in (34) are known, the diagonal elements of Z being given by (64), the remaining elements

of Z by (52), V_N^a by (68), and the remaining elements of \vec{V}^a by (74). Next, (34) is solved for \vec{I}^a . The coefficients $\{I_j^a\}$ will then be the elements of \vec{I}^a .

VII. EVALUATION OF THE MAGNETIC CURRENT COEFFICIENT V FOR TM PLANE WAVE EXCITATION

In this section, the coefficient V that appears in (42) and (43) is evaluated for the case in which the incident electromagnetic field $(\underline{E}^{inc}, \underline{H}^{inc})$ is the TM plane wave given by (44) and (45), the electric current expansion functions $\{\underline{J}_j\}$ are given by (46), and the magnetic current expansion function \underline{M}_1 is given by (47). To solve (10) for V , we must first evaluate Y^a , Y^b , and I . Here, Y^a is given by (38), Y^b by (41), and I by (28). The next eight paragraphs are devoted to evaluating Y^a .

Expression (38) for Y^a is recast as

$$Y^a = Y^{hs} - \sum_{j=1}^N I_j^a C_j^- \quad (76)$$

where

$$Y^{hs} = - \int_{-w}^w \underline{M}_1 \cdot \underline{H}(0, 2\underline{M}_1) dy \quad (77)$$

and

$$C_j^- = \int_{-w}^w \underline{M}_1 \cdot \underline{H}^-(\underline{J}_j, 0) dy \quad (78)$$

The superscript "hs" in (77) denotes half space. As defined by (77), Y^{hs} is what Y^a would be if region a were the half-space region for which $x < 0$. The truth of this statement is evident because, if region a were the half-space region for which $x < 0$, then S^{sc} would be the yz plane at $x=0$, and the split magnetic current sheet $2\underline{M}_1$ defined in the sentence that contains (29) would induce no electric current on this plane so that the summation with respect

to j in (76) would vanish.

The $\underline{H}(0, 2\underline{M}_1)$ that appears in (77) is obtained by replacing \underline{E}^s by $\underline{H}(0, 2\underline{M}_1)$, \underline{J} by $2\underline{M}_1$, μ by ϵ , and ϵ by μ in [8, eqs. (3-52) to (3-54)]. Thus,

$$\underline{H}(0, 2\underline{M}_1) = -j\omega\underline{F} - \nabla\phi \quad (79)$$

where

$$\underline{F} = \frac{\epsilon}{2j} \int_{-w}^w \underline{M}_1(y') H_0^{(2)}(k|y-y'|) dy' \quad (80)$$

and

$$\phi = \frac{1}{2\omega\mu} \int_{-w}^w \frac{dM_{1y}(y')}{dy'} H_0^{(2)}(k|y-y'|) dy' \quad (81)$$

Here, ω is the angular frequency. It has been assumed that $\underline{M}_1(y')$ exists only at $x = 0$ and has only a y component $M_{1y}(y')$. The (x, y) coordinates at which \underline{F} and ϕ are evaluated in (80) and (81) are $(0, y)$. Substitution of (79) into (77) gives

$$Y^{hs} = j\omega \int_{-w}^w \underline{M}_1(y) \cdot \underline{F} dy + \int_{-w}^w M_{1y}(y) \frac{d\phi}{dy} dy \quad (82)$$

Integrating by parts the second integral on the right-hand side of (82) and anticipating that $M_{1y}(\pm w)$ will vanish, we obtain

$$Y^{hs} = j\omega \int_{-w}^w \underline{M}_1(y) \cdot \underline{F} dy - \int_{-w}^w \frac{dM_{1y}(y)}{dy} \phi dy \quad (83)$$

If (80), (81), and (47) are substituted into (83) and if new variables of integration u and u' are defined by

$$u = y/w \quad (84)$$

$$u' = y'/w \quad (85)$$

then (83) becomes

$$Y^{hs} = \frac{(kw)^2 C_A - C_\phi}{2k\eta} \quad (86)$$

where

$$C_A = \int_{-1}^1 du \sqrt{1-u^2} \int_{-1}^1 du' \sqrt{1-(u')^2} H_0^{(2)}(kw|u-u'|) \quad (87)$$

$$C_\phi = \int_{-1}^1 du \frac{u}{\sqrt{1-u^2}} \int_{-1}^1 du' \frac{u'}{\sqrt{1-(u')^2}} H_0^{(2)}(kw|u-u'|) \quad (88)$$

Appealing to (60), we recast (87) and (88) as

$$C_A = I_A + \int_{-1}^1 du \sqrt{1-u^2} \int_{-1}^1 du' \sqrt{1-(u')^2} [H_0^{(2)}(kw|u-u'|) - 1 + \frac{j2}{\pi} \ln(\frac{\gamma kw|u-u'|}{2})] \quad (89)$$

and

$$C_\phi = I_\phi + \int_{-1}^1 du \frac{u}{\sqrt{1-u^2}} \int_{-1}^1 du' \frac{u'}{\sqrt{1-(u')^2}} [H_0^{(2)}(kw|u-u'|) - 1 + \frac{j2}{\pi} \ln(\frac{\gamma kw|u-u'|}{2})] \quad (90)$$

where

$$I_A = \int_{-1}^1 du \sqrt{1-u^2} \int_{-1}^1 du' \sqrt{1-(u')^2} [1 - \frac{j2}{\pi} \ln(\frac{\gamma kw|u-u'|}{2})] \quad (91)$$

and

$$I_\phi = \int_{-1}^1 du \frac{u}{\sqrt{1-u^2}} \int_{-1}^1 du' \frac{u'}{\sqrt{1-(u')^2}} [1 - \frac{j2}{\pi} \ln(\frac{\gamma kw|u-u'|}{2})] \quad (92)$$

It is evident from [11, eqs. (A6a) and (A6c)] that

$$\int_{-1}^1 \sqrt{1-(u')^2} \ln|u-u'| du' = \frac{\pi}{2} (u^2 - \frac{1}{2} - \ln 2) \quad (93)$$

From [10, Formula 350.01.], we obtain

$$\int_{-1}^1 \sqrt{1 - (u')^2} du' = \frac{\pi}{2} \quad (94)$$

From [10, Formula 352.01.], we obtain

$$\int_{-1}^1 u^2 \sqrt{1 - u^2} du = \frac{\pi}{8} \quad (95)$$

Equations (93) - (95) are used to reduce (91) to

$$I_A = \frac{\pi^2}{4} + \frac{j\pi}{2} \left(\frac{1}{4} - \ln \left(\frac{\gamma_{kw}}{4} \right) \right) \quad (96)$$

It is evident from [11, Eq. (A6b)] that

$$\int_{-1}^1 \frac{u'}{\sqrt{1 - (u')^2}} \ln |u - u'| du' = -\pi u \quad (97)$$

It is evident from [10, Formula 322.01.] that

$$\int_{-1}^1 \frac{u^2}{\sqrt{1 - u^2}} du = \frac{\pi}{2} \quad (98)$$

Equations (97) and (98) are used to reduce (92) to

$$I_\phi = j\pi \quad (99)$$

Now, the Y^{hs} that appears in expression (76) for Y^a is given by (86) in which C_A and C_ϕ are given by (89) and (90), respectively. In (89) and (90), I_A and I_ϕ are given by (96) and (99), respectively. The double integrals that appear explicitly in (89) and (90) are evaluated by the method of two-dimensional Gaussian quadrature.

The C_j^- that appears in expression (76) for Y^a is given by (78). In (78), the y component of $\underline{H}^-(\underline{J}_N, 0)$ is called $H_y^-(\underline{J}_N, 0)$. Since \underline{J}_N is \underline{u}_z

on the shorting strip, it follows that, at $x=0^-$,

$$H_y^-(J_N, 0) = \begin{cases} -0.5, & -w \leq y < w \\ 0, & |y| > w \end{cases} \quad (100)$$

Substitution of (47) and (100) into (78) gives

$$C_N^- = -\frac{1}{2} \int_{-w}^w \sqrt{1 - \left(\frac{y}{w}\right)^2} dy \quad (101)$$

Expressing the integral in (101) as the product of w with the integral in (94), we obtain

$$C_N^- = -\frac{\pi w}{4} \quad (102)$$

Striving to evaluate C_j^- for $j \neq N$, we let the y component of $\underline{H}(J_j, 0)$ be $H_y(J_j, 0)$ and express it as [8, eqs. (3-26) and (3-32)]

$$H_y(J_j, 0) = \underline{u}_y \cdot \nabla \times \frac{1}{4j} \int_0^{t_{N+1}} \underline{J}_j(t') H_0^{(2)}(k \sqrt{(x-x')^2 + (y-y')^2}) dt' \quad (103)$$

where (x, y) are the rectangular coordinates of the point at which $H_y(J_j, 0)$ is evaluated, and (x', y') are the rectangular coordinates of the point on the contour of S^{sc} at which the arc length is t' . In (103), " $\nabla \times$ " is the curl operator with respect to the coordinates (x, y) . If (x', y') never coincides with (x, y) , then the curl operator can be taken under the integral sign in (103). Taking the curl operator under the integral sign, substituting (46) into (103), and using [9, eqs. (A-14) and (D-15)], we obtain

$$H_y(J_j, 0) = -\frac{jk}{4} \int_{t_j}^{t_{j+1}} \frac{(x-x') H_1^{(2)}(k \sqrt{(x-x')^2 + (y-y')^2})}{\sqrt{(x-x')^2 + (y-y')^2}} dt' \quad (104)$$

Substitution of (47) and (104) into (78) gives

$$C_j^- = \frac{jk}{4} \int_{-w}^w dy \sqrt{1-(y/w)^2} \int_{t_j}^{t_{j+1}} \frac{dt' x' H_1^{(2)}(k \sqrt{(x')^2 + (y-y')^2})}{\sqrt{(x')^2 + (y-y')^2}}, \quad j \neq N \quad (105)$$

If new variables of integration u and u' are defined by

$$u = ky \quad (106)$$

$$u' = k(t' - 0.5(t_j + t_{j+1})) \quad (107)$$

then (105) becomes

$$C_j^- = \frac{j}{4k} \int_{-kw}^{kw} du \sqrt{1 - \left(\frac{u}{kw}\right)^2} \int_{-0.5\gamma_j}^{0.5\gamma_j} \frac{du' (kx_j^+ + u' \cos \phi_j) H_1^{(2)}(\alpha_{Nj})}{\alpha_{Nj}}, \quad j \neq N \quad (108)$$

where γ_j , x_j^+ , $\cos \phi_j$, and α_{Nj} are given by (53), (55), (57), and (54), respectively. The double integral on the right-hand side of (108) is the double integral on the right-hand side of (74) with i replaced by j , with u and u' interchanged, and with the order of integration interchanged.

Therefore,

$$C_j^- = -\frac{1}{2} V_j^a, \quad j=1,2,\dots,N-1 \quad (109)$$

where V_j^a is given by the right-hand side of (74) with i replaced by j .

Now, the $\{C_j^-\}$ that appear in expression (76) for Y^a are given by (109) and (102). The evaluation of the Y^{hs} that appears in (76) was described in the paragraph that follows (99). The coefficients $\{I_j^a\}$ that appear in (76) were evaluated in Section VI. This concludes our description of the evaluation of Y^a .

Expression (41) for Y^b is recast as

$$Y^b = Y^{hs} - \sum_{j=1}^N I_j^a C_j^+ \quad (110)$$

where Y^{hs} is given by (77) and C_j^+ is given by

$$C_j^+ = \int_{-w}^w \underline{M}_1 \cdot \underline{H}^+(\underline{J}_j, 0) dy \quad (111)$$

In (111), the y component of $\underline{H}^+(\underline{J}_N, 0)$ is called $H_y^+(\underline{J}_N, 0)$. Since \underline{J}_N is \underline{u}_z on the shorting strip, it follows that, at $x = 0^+$

$$H_y^+(\underline{J}_N, 0) = \begin{cases} 0.5, & -w \leq y < w \\ 0, & |y| > w \end{cases} \quad (112)$$

Now, H_y^+ of (112) is the negative of H_y^- of (100). Therefore, C_N^+ of (111) is the negative of C_N^- of (102).

$$C_N^+ = -C_N^- \quad (113)$$

If $j \neq N$, then C_j^+ of (111) is equal to C_j^- of (109).

$$C_j^+ = C_j^-, \quad j = 1, 2, \dots, N-1 \quad (114)$$

Now the $\{C_j^+\}$ that appear in expression (110) for Y^b are given by (114) and (113). The quantities Y^{hs} and I_j^a on the right-hand side of (110) are the same as in (76). This concludes our description of the evaluation of Y^b .

The quantity $(Y^a + Y^b)$ appears in (10). Thanks to (109), (113), and (114), the sum of (76) and (110) reduces to

$$Y^a + Y^b = 2Y^{hs} + \sum_{j=1}^{N-1} I_j^a V_j^a \quad (115)$$

Expression (28) for I is recast as

$$I = C^{inc} + \sum_{j=1}^N I_j^{inc} C_j^- \quad (116)$$

where C_j^- is given by (78), and

$$C^{inc} = \int_{-w}^w \underline{M}_1 \cdot \underline{H}^{inc} dy \quad (117)$$

Substituting (45) and (47) into (117) and then introducing the new variable of integration u defined by (84), we obtain

$$C^{inc} = \frac{w}{\eta} \cos \phi^{inc} \int_{-1}^1 \sqrt{1-u^2} \cos(kw u \sin \phi^{inc}) du \quad (118)$$

The integral in (118) is evaluated by the method of Gaussian quadrature.

Now, the quantity I that appears in (10) is given by (116) in which C^{inc} is given by (118), the $\{C_j^-\}$ are given by (109) and (102), and the $\{I_j^{inc}\}$ were evaluated in Section VI. The quantity $(Y^a + Y^b)$ that appears in (10) is given by (115) in which Y^{hs} is evaluated as described in the paragraph that follows (99), the $\{I_j^a\}$ were evaluated in Section VI, and V_j^a is given by (74) with i replaced by j. After I and $(Y^a + Y^b)$ have been evaluated, (10) can be solved for V.

VIII. NUMERICAL RESULTS FOR A SLOTTED TM CIRCULAR CYLINDRICAL SURFACE

In this section, numerical results are presented for the magnetic current coefficient V for the slotted TM cylindrical surface shown in Fig. 6 with

$$\left. \begin{aligned} ka &= \pi/2 \\ \phi_0 &= 5^\circ \end{aligned} \right\} \quad (119)$$

In (44), ϕ^{inc} is set equal to 180° so that the incident electric field $\underline{E}^{\text{inc}}$ is given by

$$\underline{E}^{\text{inc}} = \underline{u}_2 e^{-jkx} \quad (120)$$

The coefficient V was calculated by three different methods, the method of solution with pseudo-image, the method of solution without pseudo-image, and the Fourier series method of solution. The method of solution with pseudo-image is the method of solution described in Sections III to VII. This method was applied using 10-point Gaussian quadrature whenever Gaussian quadrature was called for, dividing the circular arc of Fig. 6 into 35 small arcs each of angular extent 10° , and replacing each of these arcs by the straight line segment joining its end points. The method of solution without pseudo-image is described in Appendix A, and the Fourier series method of solution is described in Appendix B. All three methods of solution were implemented by means of computer programs which will be described and listed in a forthcoming report.

The method of solution without pseudo-image differs from the method of solution described in Sections III to VII in that the pseudo-image of Section V is eliminated. That is, the short-circuit fields due to the magnetic current expansion function \underline{M}_1 placed on the left-hand side of the

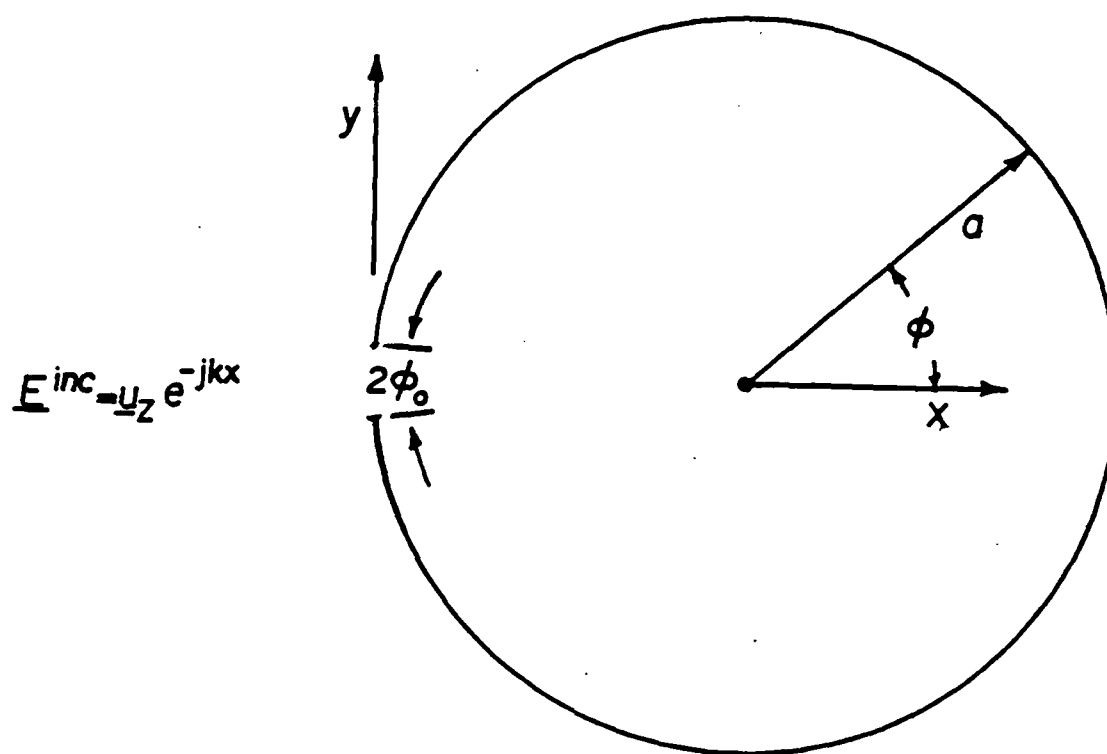


Fig. 6. The slotted TM cylindrical surface as viewed in the xy plane. It is an infinitesimally thin perfectly conducting circular cylindrical shell of radius a centered at $(x = a \cos \phi_0, y = 0)$ with a slot of angular width $2\phi_0$. The edges of the shell are at $(x = 0, y = \pm a \sin \phi_0)$. $ka = \pi/2$ and $\phi_0 = 5^\circ$.

shorted aperture are obtained by solving the scattering problem of Fig. 4 rather than that of Fig. 5. Similarly, the short-circuit fields due to \underline{M}_1 placed on the right-hand side of the shorted aperture are obtained by solving the scattering problem not of Fig. 5 but of the situation that would exist in Fig. 4 if \underline{M}_1 were placed on the right-hand side of the shorted aperture instead of on the left-hand side of it.

In the Fourier series method of solution, the aperture electric field \underline{E} rather than the magnetic current \underline{M} is expanded. Furthermore, \underline{E} is expanded not on the straight line connects the end points ($x = 0, y = \pm a \sin \phi_0$) of the circular arc in Fig. 6, but on the circular arc of angular extent $2\phi_0$ that connects these end points. The combination of this circular arc of angular extent $2\phi_0$ and the existing circular arc in Fig. 6 would form a complete circle. In the Fourier series method of solution,

$$\underline{E}(\phi) = -V \underline{u}_z \sqrt{1 - \left(\frac{\phi - 180^\circ}{\phi_0}\right)^2}, \quad -\phi_0 \leq \phi - 180^\circ \leq \phi_0 \quad (121)$$

where V is an unknown complex constant to be evaluated and ϕ is the angle shown in Fig. 6. If the y axis passed through the center of the circle whose arc appears in Fig. 6, then ϕ would be the usual cylindrical coordinate angle measured in the counterclockwise direction from the positive x axis. In (121), $\underline{E}(\phi)$ is the electric field on the circular arc of extent $2\phi_0$ needed to complete the circle in Fig. 6. Therefore, the (x,y) coordinates of the location of $\underline{E}(\phi)$ are given by

$$\left. \begin{aligned} x &= a(\cos \phi_0 + \cos \phi) \\ y &= a \sin \phi \end{aligned} \right\} \quad (122)$$

To compare the method of solution with pseudo-image to the Fourier series method of solution, we must interpret \underline{M} of (9) in terms of the electric field \underline{E} in the slot. Combining (1) with (9) and assuming that \underline{E} has no component in the x direction, we obtain

$$\underline{E} = -V \underline{u}_x \times \underline{M}_1 \quad (123)$$

Substitution of (47) into (123) gives

$$\underline{E}(y) = -V \underline{u}_z \sqrt{1 - (y/w)^2}, \quad -w \leq y \leq w \quad (124)$$

No confusion should arise from the fact that the argument of \underline{E} of (124) is a rectangular coordinate whereas that of \underline{E} of (121) is an angle. The \underline{E} of (124) is the electric field at $x = 0$ in the slot, but the \underline{E} of (121) is the electric field on the circular arc of angular extent $2\phi_0$ needed to complete the circle in Fig. 6. The (x,y) coordinates on this circular arc are given in terms of ϕ by (122).

Calculated values of V are presented in Table 1. In Table 1, the phases of V are nearly the same, differing by 0.24° at most. The phase lead of 0.21° for the V obtained by the Fourier series method of solution with respect to the V obtained by the method of solution with pseudo-image is reasonable because it is shown as follows that the phase of \underline{E}^{inc} at the location of $\underline{E}(180^\circ)$ of (121) is 0.342° and that the phase of \underline{E}^{inc} at the location of $\underline{E}(0)$ of (124) is 0° . According to the first of equations (122) and the second of equations (119), the x coordinate of the location of $\underline{E}(180^\circ)$ of (121) is given by

$$x = -0.0038a \quad (125)$$

Thanks to the first of equations (119), the phase of \underline{E}^{inc} of (120) is 0.342° when x is given by (125). Therefore, the phase of \underline{E}^{inc} at the location of $\underline{E}(180^\circ)$ of (121) is 0.342° . The x coordinate of the location of $\underline{E}(0)$ of (124) is zero. At $x = 0$, the phase of \underline{E}^{inc} of (120) is 0° . Therefore, the phase of \underline{E}^{inc} at the location of $\underline{E}(0)$ of (124) is 0° .

Table 1. The coefficient V for the slotted TM circular cylindrical surface shown in Fig. 6.

Method of solution	Real part of V	Imaginary part of V	Magnitude of V	Phase of V in degrees
With pseudo-image	-0.0347	-0.1483	0.1523	-103.17
Without pseudo-image	-0.0399	-0.1701	0.1747	-103.20
Fourier series	-0.0344	-0.1495	0.1534	-102.96

In Table 1, the magnitude of the V obtained by the method of solution with pseudo-image is a trifle smaller than that of the V obtained by the Fourier series method of solution. This is expected because the location of $\underline{E}(0)$ of (124) is slightly inside the circular arc in Fig. 6 as compared to the location of $\underline{E}(180^\circ)$ of (121). The electric field should decrease as the interior of an aperture perforated cavity is approached.

In Table 1, the complex number V obtained by the method of solution with pseudo-image agrees well with that obtained by the Fourier series method of solution. However, the magnitude of the complex number V obtained by the method of solution without pseudo-image is more than 10% too large. In this case, the complex number V obtained by the method of solution with pseudo-image is evidently more accurate than that obtained

by the method of solution without pseudo-image. We believe that, for scattering problems involving small apertures, the method of solution with pseudo-image gives results that are generally more accurate than those obtained by the method of solution without pseudo-image. More computations are presently being done in order to verify this belief.

APPENDIX A

THE METHOD OF SOLUTION WITHOUT PSEUDO-IMAGE

Calculation of the magnetic current coefficient V by means of the method of solution without pseudo-image is described in this appendix. Equation (10) can be solved for V if the quantities Y^a , Y^b , and I are known. In the method of solution without pseudo-image, the short-circuit magnetic field $\underline{H}^a(0, \underline{M}_1)$ in expression (11) for Y^a is obtained by solving the scattering problem of Fig. 4 rather than that of Fig. 5. Moreover, the short-circuit magnetic field $\underline{H}^b(0, \underline{M}_1)$ in expression (12) for Y^b is obtained by solving the scattering problem not of Fig. 5 but of the situation that would exist in Fig. 4 if \underline{M}_1 were placed on the right-hand side of the shorted aperture instead of on the left-hand side of it. Furthermore, the quantity I in (10) is the same as obtained by the method of solution with pseudo-image.

Considering the situation of Fig. 4 rather than that of Fig. 5, we write, instead of (29) and (30),

$$\underline{E}^a(0, \underline{M}_1) = \underline{E}(0, \underline{M}_1^-) + \underline{E}(\underline{J}^{aw}, 0) \quad \text{in region a} \quad (\text{A-1})$$

and

$$\underline{H}^a(0, \underline{M}_1) = \underline{H}(0, \underline{M}_1^-) + \underline{H}(\underline{J}^{aw}, 0) \quad \text{in region a} \quad (\text{A-2})$$

where \underline{J}^{aw} is the electric current induced on S^{sc} in Fig. 4. The "w" in the superscript "aw" means without pseudo-image. The superscript "-" on \underline{M}_1 on the right-hand sides of (A-1) and (A-2) indicates that \underline{M}_1 is placed on the left-hand side of the shorted aperture. Analogous to (33), \underline{J}^{aw} is approximated by

$$\underline{J}^{aw} = \sum_{j=1}^N I_j^{aw} \underline{J}_j \quad (A-3)$$

so that (34) is replaced by

$$\sum \underline{I}^{aw} = \underline{V}^{aw} \quad (A-4)$$

where the j th element of \underline{I}^{aw} is the constant I_j^{aw} that appears in (A-3).

The i th element of \underline{V}^{aw} is given by

$$V_i^{aw} = \int_0^{t_{N+1}} \underline{J}_i \cdot \underline{E}(0, \underline{M}_1^-) dt \quad (A-5)$$

Substitution of (A-3) into (A-2) gives

$$\underline{H}^a(0, \underline{M}_1) = \underline{H}(0, \underline{M}_1^-) + \sum_{j=1}^N I_j^{aw} \underline{H}(\underline{J}_j, 0) \quad \text{in region a} \quad (A-6)$$

Substituting (A-6) into (11) with Y^a replaced by Y^{aw} where the extra superscript "w" means without pseudo-image, we obtain

$$Y^{aw} = \frac{1}{2} Y^{hs} - \sum_{j=1}^N I_j^{aw} C_j^- \quad (A-7)$$

where Y^{hs} is given by (77) and C_j^- by (78).

Consider the situation that would exist if \underline{M}_1 was on the right-hand side of the shorted aperture in Fig. 4 instead of on the left-hand side of it. In this situation, the electromagnetic field ($\underline{E}^b(0, \underline{M}_1)$, $\underline{H}^b(0, \underline{M}_1)$) is given by

$$\underline{E}^b(0, \underline{M}_1) = \underline{E}(0, \underline{M}_1^+) + \underline{E}(\underline{J}^{bw}, 0) \quad \text{in region b} \quad (A-8)$$

$$\underline{H}^b(0, \underline{M}_1) = \underline{H}(0, \underline{M}_1^+) + \underline{H}(\underline{J}^{bw}, 0) \quad \text{in region b} \quad (A-9)$$

where \underline{J}^{bw} is the electric current induced on S^{sc} in the previously described situation. In the superscript "bw" the "b" denotes the electromagnetic field problem in region b, and the "w" means without pseudo-image.

The superscript "+" on \underline{M}_1 on the right-hand sides of (A-8) and (A-9) indicates that \underline{M}_1 is placed on the right-hand side of the shorted aperture. Analogous to (33), \underline{J}^{bw} is approximated by

$$\underline{J}^{bw} = \sum_{j=1}^N \underline{I}_j^{bw} \underline{J}_j \quad (\text{A-10})$$

Using the method of moments to solve the electromagnetic field problem, we obtain the following matrix equation which is similar to (34).

$$\underline{Z} \underline{I}^{bw} = \underline{V}^{bw} \quad (\text{A-11})$$

The j th element of \underline{I}^{bw} is the constant \underline{I}_j^{bw} that appears in (A-10). The i th element of \underline{V}^{bw} is given by

$$\underline{V}_i^{bw} = \int_0^{t_{N+1}} \underline{J}_i \cdot \underline{E}(0, \underline{M}_1^+) dt \quad (\text{A-12})$$

Substitution of (A-10) into (A-9) gives

$$\underline{H}^b(0, \underline{M}_1) = \underline{H}(0, \underline{M}_1^+) + \sum_{j=1}^N \underline{I}_j^{bw} \underline{H}(\underline{J}_j, 0) \quad \text{in region } b \quad (\text{A-13})$$

Substituting (A-13) into (12) with \underline{Y}^b replaced by \underline{Y}^{bw} where the extra superscript "w" means without pseudo-image, we obtain

$$\underline{Y}^{bw} = \frac{1}{2} \underline{Y}^{hs} - \sum_{j=1}^N \underline{I}_j^{bw} \underline{C}_j^+ \quad (\text{A-14})$$

where \underline{Y}^{hs} is given by (77) and \underline{C}_j^+ by (111).

The sum of (A-7) and (A-14) is

$$\underline{Y}^{aw} + \underline{Y}^{bw} = \underline{Y}^{hs} - \sum_{j=1}^N (\underline{I}_j^{aw} \underline{C}_j^- + \underline{I}_j^{bw} \underline{C}_j^+) \quad (\text{A-15})$$

Because \underline{C}_j^- is given by (102) and (109) and \underline{C}_j^+ is given in terms of \underline{C}_j^-

by (113) and (114), (A-15) becomes

$$Y^{aw} + Y^{bw} = Y^{hs} + \frac{\pi w}{4} (I_N^{aw} - I_N^{bw}) + \frac{1}{2} \sum_{j=1}^{N-1} (I_j^{aw} + I_j^{bw}) V_j^a \quad (A-16)$$

The sum of (A-4) and (A-11) is

$$Z[\vec{I}^{aw} + \vec{I}^{bw}] = \vec{V}^{aw} + \vec{V}^{bw} \quad (A-17)$$

It is evident from (A-5), (A-12), and (35) that

$$\vec{V}^{aw} + \vec{V}^{bw} = \vec{V}^a \quad (A-18)$$

Substituting (A-18) into (A-17) and comparing the result with (34), we obtain

$$I_j^{aw} + I_j^{bw} = I_j^a, \quad j=1,2,\dots,N \quad (A-19)$$

Equation (A-19) is true because the sum of the electromagnetic sources in the field problems whose matrix equations are (A-4) and (A-11) is the electromagnetic source in the field problem whose matrix equation is (34).

Subtracting (A-11) from (A-4), we obtain

$$Z[\vec{I}^{aw} - \vec{I}^{bw}] = \vec{V}^{aw} - \vec{V}^{bw} \quad (A-20)$$

The difference between (A-5) and (A-12) is

$$V_i^{aw} - V_i^{bw} = \int_0^{t_{N+1}} \underline{J}_i \cdot (\underline{E}(0, \underline{M}_1^-) - \underline{E}(0, \underline{M}_1^+)) dt \quad (A-21)$$

Because \underline{M}_1^- is \underline{M}_1 placed on the left-hand side of the shorted aperture and \underline{M}_1^+ is \underline{M}_1 placed on the right-hand side of the shorted aperture where \underline{M}_1 is given by (47), the difference field in (A-21) exists only at $x = 0$ between the magnetic current sheets \underline{M}_1^- and \underline{M}_1^+ where it is given by

$$\underline{E}(0, \underline{M}_1^-) - \underline{E}(0, \underline{M}_1^+) = \underline{u}_2 \sqrt{1 - (y/w)^2} \quad (\text{A-22})$$

Substituting (A-22) and (46) into (A-21) and using (94), we obtain

$$\left. \begin{aligned} v_i^{aw} - v_i^{bw} &= 0, \quad i = 1, 2, \dots, N-1 \\ v_N^{aw} - v_N^{bw} &= \frac{\pi w}{2} \end{aligned} \right\} \quad (\text{A-23})$$

Substitution of (A-19) into (A-16) gives

$$Y^{aw} + Y^{bw} = Y^{hs} + \frac{\pi w}{4} (I_N^{aw} - I_N^{bw}) + \frac{1}{2} \sum_{j=1}^{N-1} I_j^a v_j^a \quad (\text{A-24})$$

where, from what was done in the previous paragraph, $(I_N^{aw} - I_N^{bw})$ is the Nth element of the solution $[\vec{I}^{aw} - \vec{I}^{bw}]$ to (A-20) when the elements of $[\vec{V}^{aw} - \vec{V}^{bw}]$ are given by (A-23). Comparison of (A-24) with (115) gives

$$Y^{aw} + Y^{bw} = \frac{1}{2} (Y^a + Y^b) + \frac{\pi w}{4} (I_N^{aw} - I_N^{bw}) \quad (\text{A-25})$$

Affixing the superscript "w" to all quantities on the left-hand side of (10) to indicate without pseudo-image, and solving the resulting equation for V^w , we obtain

$$V^w = I / (Y^{aw} + Y^{bw}) \quad (\text{A-26})$$

where V^w is the magnetic current coefficient obtained by the method of solution without pseudo-image and $(Y^{aw} + Y^{bw})$ is given by (A-25).

APPENDIX B

THE FOURIER SERIES METHOD OF SOLUTION FOR A SLOTTED TM CIRCULAR CYLINDRICAL SURFACE

In this appendix, the Fourier series method of solution is used to solve the scattering problem that arises when the electric field $\underline{E}^{\text{inc}}$ of (120) is incident on the conducting surface in Fig. 6. We require that E_z be continuous at $\rho=a$ where E_z is the z component of the electric field and ρ is the distance from the center of the circle whose arc appears in Fig. 6. Combining (121) with the fact that E_z vanishes on the circular arc in Fig. 6, we obtain

$$E_z = \begin{cases} -V \sqrt{1 - \left(\frac{\phi - 180^\circ}{\phi_0}\right)^2}, & -\phi_0 \leq \phi - 180^\circ \leq \phi_0 \\ 0 & , \text{ other values of } \phi \end{cases} \quad (\text{B-1})$$

at $\rho=a$. If the y axis passed through the center of the circle whose arc appears in Fig. 6, then ϕ would be the usual cylindrical coordinate angle measured in the counterclockwise direction from the positive x axis. Since E_z is constrained by (B-1), the ϕ component of the magnetic field can not be continuous across the entire circular arc of angular extent $2\phi_0$ that bridges the gap to form a complete circle in Fig. 6. However, the ϕ component of the magnetic field can satisfy

$$\int_{180^\circ - \phi_0}^{180^\circ + \phi_0} (H_\phi^+ - H_\phi^-) \sqrt{1 - \left(\frac{\phi - 180^\circ}{\phi_0}\right)^2} d\phi = 0 \quad (\text{B-2})$$

where H_ϕ^- is the limit as ρ approaches a from below of the ϕ component of the magnetic field and H_ϕ^+ is the limit as ρ approaches a from above of the

ϕ component of the magnetic field. In what follows, E_z is expanded in separate Fourier series in the regions for which $\rho < a$ and $\rho > a$, E_z is required to be continuous at $\rho=a$, and E_z is forced to conform with (B-1) at $\rho=a$. Finally, (B-2) is used to determine the unknown complex constant V that appears in (B-1).

In the region for which $\rho > a$, the Fourier series expansion for E_z consists of the Fourier series expansion of E_z^{inc} and a sum of outward-traveling waves. Here, E_z^{inc} is the z component of the incident electric field. The x coordinate that appears in expression (120) for E_z^{inc} is expressed in terms of ρ and ϕ as

$$x = a \cos \phi_0 + \rho \cos \phi \quad (B-3)$$

Substituting (B-3) into (120), and then taking the z component of the resulting equation, we obtain

$$E_z^{inc} = e^{-jka \cos \phi_0} e^{-jk\rho \cos \phi} \quad (B-4)$$

If [9, eq. (5-101)] is used to expand the second exponential in (B-4), then (B-4) becomes

$$E_z^{inc} = e^{-jka \cos \phi_0} \sum_{n=-\infty}^{\infty} j^{-n} J_n(k\rho) e^{jn\phi} \quad (B-5)$$

where J_n is the Bessel function of the first kind of order n .

Since E_z is finite at $\rho = 0$, the Fourier series expansion for E_z in the region for which $\rho < a$ can have only Bessel functions of the first kind. Moreover, the Fourier series expansion for E_z in the region for which $\rho > a$ consists of E_z^{inc} of (B-5) and a sum of outward traveling waves. Therefore,

$$E_z = \begin{cases} e^{-jka \cos \phi_0} \sum_{n=-\infty}^{\infty} A_n J_n(k\rho) e^{jn\phi}, & \rho < a \\ e^{-jka \cos \phi_0} \sum_{n=-\infty}^{\infty} (j^{-n} J_n(k\rho) + B_n H_n^{(2)}(k\rho)) e^{jn\phi}, & \rho > a \end{cases} \quad (B-6)$$

where $H_n^{(2)}$ is the Hankel function of the second kind of order n , and A_n and B_n are unknown complex constants. Requiring E_z of (B-6) to be continuous at $\rho=a$, we obtain

$$B_n = \frac{(A_n - j^{-n})J_n(ka)}{H_n^{(2)}(ka)} \quad (B-7)$$

Substitution of (B-7) into (B-6) gives

$$E_z = \begin{cases} e^{-jka \cos \phi_0} \sum_{n=-\infty}^{\infty} A_n J_n(k\rho) e^{jn\phi} & , \rho \leq a \\ e^{-jka \cos \phi_0} \sum_{n=-\infty}^{\infty} (j^{-n} J_n(k\rho) + \frac{(A_n - j^{-n}) J_n(ka)}{H_n^{(2)}(ka)} H_n^{(2)}(k\rho)) e^{jn\phi} & , \rho \geq a \end{cases} \quad (B-8)$$

Requiring the upper right-hand side of (B-8) at $\rho=a$ to be equal to the right-hand side of (B-1), we obtain

$$e^{-jka \cos \phi_0} \sum_{m=-\infty}^{\infty} A_m J_m(ka) e^{jm\phi} = \begin{cases} -v \sqrt{1 - \left(\frac{\phi - 180^\circ}{\phi_0}\right)^2} & , -\phi_0 \leq \phi - 180^\circ \leq \phi_0 \\ 0 & , \text{other values of } \phi \end{cases} \quad (B-9)$$

The new summation index m in (B-9) was chosen for convenience. Multiplying both sides of (B-9) by $e^{-jn\phi}$ and integrating from 0 to 2π with respect to ϕ , we obtain

$$2\pi A_n J_n(ka) e^{-jka \cos \phi_0} = -v \int_{180^\circ - \phi_0}^{180^\circ + \phi_0} \sqrt{1 - \left(\frac{\phi - 180^\circ}{\phi_0}\right)^2} e^{-jn\phi} d\phi \quad (B-10)$$

If the quantity in parentheses on the right-hand side of (B-10) is called x , then (B-10) reduces to

$$2\pi A_n J_n(ka) e^{-jka \cos \phi_0} = -v \phi_0 (-1)^n \int_{-1}^1 \sqrt{1-x^2} \cos(n\phi_0 x) dx \quad (B-11)$$

According to [12, Formula 3.752 (2.)],

$$\int_{-1}^1 \sqrt{1-x^2} \cos(n\phi_0 x) dx = \pi \frac{J_1(|n|\phi_0)}{|n|\phi_0} \quad (\text{B-12})$$

Equation (B-12) is written with the understanding that $J_1(|n|\phi_0)/(|n|\phi_0)$ is to be replaced by 1/2 when n is zero. Substitution of (B-12) into (B-11) leads to

$$A_n J_n(ka) e^{-jka \cos \phi_0} = - \frac{V\phi_0 (-1)^n}{2} \left(\frac{J_1(|n|\phi_0)}{|n|\phi_0} \right) \quad (\text{B-13})$$

Substituting (B-13) into (B-8), we obtain

$$E_z = \begin{cases} - \frac{V\phi_0}{2} \sum_{n=-\infty}^{\infty} \frac{(-1)^n}{J_n(ka)} \left(\frac{J_1(|n|\phi_0)}{|n|\phi_0} \right) J_n(k\rho) e^{jn\phi} & , \quad \rho \leq a \\ - \frac{V\phi_0}{2} \sum_{n=-\infty}^{\infty} \frac{(-1)^n}{H_n^{(2)}(ka)} \left(\frac{J_1(|n|\phi_0)}{|n|\phi_0} \right) H_n^{(2)}(k\rho) e^{jn\phi} + \\ e^{-jka \cos \phi_0} \sum_{n=-\infty}^{\infty} j^{-n} \left(J_n(k\rho) - \frac{J_n(ka)}{H_n^{(2)}(ka)} H_n^{(2)}(k\rho) \right) e^{jn\phi} & , \quad \rho \geq a \end{cases} \quad (\text{B-14})$$

With a view toward enforcing (B-2), we call the ϕ component of the magnetic field H_ϕ and express it as [9, eq. (5-18)]

$$H_\phi = -\frac{j}{k\eta} \frac{\partial E_z}{\partial \rho} \quad (\text{B-15})$$

The limits of (B-15) as ρ approaches a from below and above are

$$H_\phi^- = -\frac{j}{k\eta} \lim_{\rho \rightarrow a^-} \frac{\partial E_z}{\partial \rho} \quad (\text{B-16})$$

and

$$H_\phi^+ = -\frac{j}{k\eta} \lim_{\rho \rightarrow a^+} \frac{\partial E_z}{\partial \rho} \quad (\text{B-17})$$

where $\lim_{\rho \rightarrow a^-}$ and $\lim_{\rho \rightarrow a^+}$ denote the limits as ρ approaches a from below and above, respectively. Substitution of (B-14) into (B-16) and (B-17) gives

$$H_{\phi}^{-} = \frac{jV\phi_o}{2\eta} \sum_{n=-\infty}^{\infty} \frac{(-1)^n}{J_n(ka)} \left(\frac{J_1(|n|\phi_o)}{|n|\phi_o} \right) J_n'(ka) e^{jn\phi} \quad (B-18)$$

and

$$H_{\phi}^{+} = \frac{jV\phi_o}{2\eta} \sum_{n=-\infty}^{\infty} \frac{(-1)^n}{H_n^{(2)}(ka)} \left(\frac{J_1(|n|\phi_o)}{|n|\phi_o} \right) H_n^{(2)'}(ka) e^{jn\phi} -$$

$$\frac{j}{\eta} e^{-jka \cos \phi_o} \sum_{n=-\infty}^{\infty} j^{-n} \left(J_n'(ka) - \frac{J_n(ka)}{H_n^{(2)}(ka)} H_n^{(2)'}(ka) \right) e^{jn\phi} \quad (B-19)$$

The identity [9, eqs. (D-12) and (D-17)]

$$J_n(x) H_n^{(2)'}(x) - J_n'(x) H_n^{(2)}(x) = -\frac{2j}{\pi x} \quad (B-20)$$

reduces the difference of (B-18) and (B-19) to

$$H_{\phi}^{+} - H_{\phi}^{-} = \frac{V\phi_o}{\pi\eta ka} \sum_{n=-\infty}^{\infty} (-1)^n \left(\frac{J_1(|n|\phi_o)}{|n|\phi_o} \right) \left(\frac{1}{J_n(ka) H_n^{(2)}(ka)} \right) e^{jn\phi} +$$

$$\frac{2}{\pi\eta ka} e^{-jka \cos \phi_o} \sum_{n=-\infty}^{\infty} \frac{j^{-n} e^{jn\phi}}{H_n^{(2)}(ka)} \quad (B-21)$$

Substitution of (B-21) into (B-2) and use of the identity

$$\int_{180^\circ - \phi_o}^{180^\circ + \phi_o} \sqrt{1 - \left(\frac{\phi - 180^\circ}{\phi_o} \right)^2} e^{jn\phi} d\phi = \pi\phi_o (-1)^n \left(\frac{J_1(|n|\phi_o)}{|n|\phi_o} \right) \quad (B-22)$$

lead to

$$V = - \frac{2e^{-jka \cos \phi_0} \sum_{n=-\infty}^{\infty} \frac{j^n}{H_n^{(2)}(ka)} \left(\frac{J_1(n\phi_0)}{n\phi_0} \right)}{\phi_0 \sum_{n=-\infty}^{\infty} \frac{1}{J_n(ka) H_n^{(2)}(ka)} \left(\frac{J_1(n\phi_0)}{n\phi_0} \right)^2} \quad (B-23)$$

The identity (B-22) was obtained by noting that the value of the integral on the left-hand side of (B-22) is the same as the value of the integral on the right-hand side of (B-10) and by determining this common value by comparing (B-13) with (B-10). Recalling that $J_1(n\phi_0)/(n\phi_0)$ is to be replaced by 1/2 when $n = 0$ and using the identities [13, Formulas 9.1.5 and 9.1.6]

$$\left. \begin{aligned} J_{-n}(x) &= (-1)^n J_n(x) \\ H_{-n}^{(2)}(x) &= (-1)^n H_n^{(2)}(x) \end{aligned} \right\} \quad (B-24)$$

each term for which n is a negative integer in the sums on the right-hand side of (B-23) can be combined with the term for which n is the positive integer of the same magnitude. Thus, (B-23) becomes

$$V = - \frac{2e^{-jka \cos \phi_0} \left[\frac{1}{4 H_0^{(2)}(ka)} + \sum_{n=1}^{\infty} \frac{j^n}{H_n^{(2)}(ka)} \left(\frac{J_1(n\phi_0)}{n\phi_0} \right) \right]}{\phi_0 \left[\frac{1}{8 J_0(ka) H_0^{(2)}(ka)} + \sum_{n=1}^{\infty} \frac{1}{J_n(ka) H_n^{(2)}(ka)} \left(\frac{J_1(n\phi_0)}{n\phi_0} \right)^2 \right]} \quad (B-25)$$

REFERENCES

- [1] A. W. Glisson and D. R. Wilton, "Simple and Efficient Numerical Methods for Problems of Electromagnetic Radiation and Scattering from Surfaces," IEEE Trans. Antennas Propagat., vol. AP-28, pp. 593-603, Sept. 1980.
- [2] S. M. Rao, D. R. Wilton, and A. W. Glisson, "Electromagnetic Scattering by Surfaces of Arbitrary Shape," IEEE Trans. Antennas Propagat., vol. AP-30, pp. 409-418, May 1982.
- [3] H. K. Schuman and D. E. Warren, "Aperture Coupling in Bodies of Revolution," IEEE Trans. Antennas Propagat., vol. AP-26, pp. 778-783, Nov. 1978.
- [4] R. F. Harrington and J. R. Mautz, "A Generalized Network Formulation for Aperture Problems," IEEE Trans. Antennas Propagat., vol. AP-24, pp. 870-873, Nov. 1976.
- [5] R. F. Harrington and J. R. Mautz, "Electromagnetic Transmission through an Aperture in a Conducting Plane," AEÜ, vol. 31, pp. 81-87, Feb. 1977.
- [6] C. M. Butler and K. R. Umashankar, "Electromagnetic Penetration through an Aperture in an Infinite, Planar Screen Separating Two Half Spaces of Different Electromagnetic Properties," Radio Science, vol. 11, pp. 611-619, July 1976.
- [7] E. Arvas, R. F. Harrington, and J. R. Mautz, "Radiation and Scattering from Electrically Small Conducting Bodies of Arbitrary Shape," Report SYRU/DECE/TR-83/2, Department of Electrical and Computer Engineering, Syracuse University, Syracuse, NY 13210, Jan. 1983.

- [8] R. F. Harrington, Field Computation by Moment Methods, Macmillan, New York, 1968.
- [9] R. F. Harrington, Time-Harmonic Electromagnetic Fields, McGraw-Hill, New York, 1961.
- [10] H. B. Dwight, Tables of Integrals and Other Mathematical Data, Fourth edition, Macmillan, New York, 1961.
- [11] C. M. Butler and D. R. Wilton, "General Analysis of Narrow Strips and Slots," IEEE Trans. Antennas Propagat., vol. AP-28, pp. 42-48, Jan. 1980.
- [12] I. S. Gradshteyn and I. M. Ryzhik, Table of Integrals, Series, and Products, Academic Press, New York, 1965.
- [13] M. Abramowitz and I. A. Stegun, Handbook of Mathematical Functions, U. S. Government Printing Office, Washington, D. C. (Natl. Bur. Std. U. S. Applied Math. Ser. 55), 1964.

END

FILMED

3-86

DTIC